

Reggeon diagram technique for inclusive processes in the triple-Regge limit

Henry D. I. Abarbanel and J. Bartels

*Fermi National Accelerator Laboratory, Batavia, Illinois 60510**

J. B. Bronzan† and D. Sidhu

Rutgers University, New Brunswick, New Jersey 08903

(Received 8 May 1975)

We derive rules for evaluating Regge branch-cut corrections to the triple-Regge regime of inclusive reactions. Our approach is to study classes of hybrid field-theory graphs for the six-point function and to set up a constructive procedure for evaluating the contributions with discontinuities in the missing mass. We find that all contributions, cut and pole, can be given in terms of a single partial-wave amplitude and our rules are for constructing that. The rules are then cast into a form appropriate for a Reggeon field-theory evaluation of this partial-wave amplitude, and a renormalization-group attack on the problem is outlined. This latter work is especially relevant for the case when Pomeron exchange is permitted and a nonperturbative evaluation of the partial-wave amplitude near $J_i \approx 1$ and $t_i \approx 0$ is required.

I. INTRODUCTION

Analyzing the effects of branch points in partial-wave amplitudes $F(J, t)$ and their contributions to elastic scattering amplitudes $T(s, t)$ has been an on-going project for over a decade. The initial arguments of Mandelstam,¹ Gribov, Pomeranchuk, and Ter-Martirosyan,² and of Amati, Stanghellini, and Fubini,³ emphasized the necessity of moving branch points in J given the presence of moving poles at $J = \alpha(t)$. In retrospect it can be seen that the underlying reason for the branch points is unitarity as expressed by rescattering in the s channel or by multiparticle states in the t channel.⁴

The study of branch points took on an imperative nature, at least for the Pomeron (P) which has $\alpha(0) = 1$, when the generalizations of the Finkelstein-Kajantie problem⁵ for P poles having $\alpha(t) = 1 + \alpha't$ near $t=0$ were shown to lead to the conclusion that the P must decouple from total cross sections.⁶⁻⁸ A key step in this argument⁶ involved the vanishing of the triple- P vertex, $g_P(t)$, which is measured in inclusive processes in the triple-Regge limit.

In this paper we return to the triple- P region of inclusive reactions using the recent progress^{4,9,10} in the study of branch-point contributions to elastic processes as a guide to our approach. Here we will construct a diagram technique for evaluating multi- P contributions to the partial-wave amplitude for the triple-Regge limit of the three-to-three process whose discontinuity in missing mass gives the inclusive reaction. This diagram technique will then be employed in formulating a field theory for the interacting P 's, and the solution to this field theory will be studied in the

small- $(J-1)$, small- t limit using the renormalization group for the field theory. A subsequent paper carries out the necessary additional arguments needed to transcribe the Reggeon field-theory result into its consequences for the inclusive cross section as a function of s , t , and M^2 , the missing mass.

It is worth noting that the triple- P region of single-particle inclusive reactions is only one of many important places in which to investigate the consequences of a Reggeon field theory. The issue is basically this: Reggeon field theories are constructed to automatically satisfy the t -channel Reggeon discontinuity formulas.^{4,11} There is no *a priori* guarantee that they automatically meet the requirements of unitarity in the s channel. To look into that question one can analyze in detail specific s -channel processes beyond elastic scattering. Since the Reggeon field theory that describes elastic processes is not directly applicable to inelastic reactions, such an analysis typically has to begin with the derivation of a Reggeon calculus for the specific process to be considered. Some of this has been done by Migdal *et al.*,⁹ who use an heuristic Reggeon diagram technique for multiparticle production cross sections and single-particle inclusive processes. A more complete analysis of the $2 \rightarrow N$ production amplitudes has been given by Bartels¹² and further study of those processes is being done by Bartels and Rabinovici.¹³ These studies show that the Reggeon calculus for inelastic reactions, although each process requires its own set of rules, has in all cases the same structure and is a generalization of Gribov's Reggeon calculus for the $2 \rightarrow 2$ process.

Our plan in this paper will be to begin in Sec. II

with kinematic preliminaries for the triple- P region. Then we will use the method of hybrid Feynman graphs to abstract Reggeon diagram rules for the appropriate partial-wave amplitude. After casting these rules into "covariant" form we discuss the renormalization program for the field theory and give the renormalization-group equations for the theory. The detailed structure of the inclusive cross section requires rather much more analysis which we present in the accompanying paper.

The major result of the present article is a set of Reggeon rules for single-particle inclusive processes in the triple-Regge region. We study the three-to-three amplitude T_6 of Fig. 1 in the limit

$$\begin{aligned} s_{12} &= (p_1 + p_2)^2 \rightarrow \infty, \\ s_{13} &= (p_1' + p_3')^2 \rightarrow \infty, \\ s_1 &= (p_1 + p_2 - p_2')^2 \rightarrow \infty, \\ \frac{s_{12}}{s_1} &\rightarrow \infty, \quad \frac{s_{13}}{s_1} \rightarrow \infty, \end{aligned} \quad (1)$$

with

$$\begin{aligned} \frac{s_{12}}{s_{13}}, s_{23} &= (p_3 - p_2')^2, \\ s_2 &= (p_2 + p_1 - p_1')^2, \\ s_3 &= (p_3 + p_2 - p_2')^2, \quad Q_i^2 = t_i \end{aligned} \quad (2)$$

$$T_6(s_{12}, s_{13}, s_1, Q_i^2) = \int \frac{dJ_1 dJ_2 dJ_3}{(2\pi i)^3} \xi_{J_2} \xi_{J_3} \xi_{J_1 - J_2 - J_3} \left(\frac{s_{12}}{s_1}\right)^{J_2} \left(\frac{s_{13}}{s_1}\right)^{J_3} s_1^{J_1} F(J_1, J_2, J_3, t_i), \quad (4)$$

where

$$\xi_{J_i} = \frac{e^{-i\pi J_i + \tau_i}}{\sin \pi J_i}, \quad \xi_{J_1 - J_2 - J_3} = \frac{e^{-i\pi(J_1 - J_2 - J_3) + \tau_1 \tau_2 \tau_3}}{\sin \pi(J_1 - J_2 - J_3)}, \quad (5)$$

where the τ_i are signatures in the J_i channel (Fig. 3). The function $F(J_i, t_i)$ is real analytic and is to be evaluated from the rules we now begin to formulate.

II. KINEMATIC PRELIMINARIES AND POLE GRAPH

It is now pretty well understood how cuts in J enter elastic amplitudes. The position of such

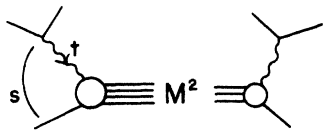


FIG. 2. The inclusive reaction with variables s , t , and M^2 . We are interested in this cross section when s , M^2 , and $s/M^2 \rightarrow \infty$, t fixed.

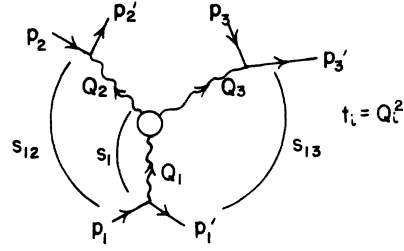


FIG. 1. Kinematics of the six-point amplitude in the triple-Regge region.

held fixed. The inclusive process is reached when $t_1 = 0$, $t_2 = t_3 = t$, and $s_{12} = s_{13} = s$ and the inclusive cross section is

$$s^2 \frac{d\sigma}{dt dM^2} = \frac{1}{2i} \text{disc}_{M^2} T_6, \quad (3)$$

where the missing mass $M^2 = s_1$ (see Fig. 2).

We find that the Reggeon pole and cut contributions to T_6 which have a missing-mass discontinuity can be written in the form

cuts and the discontinuity across them can be found on rather general grounds using multiparticle t -channel unitarity.⁴ A more pedestrian, yet very powerful, approach was used by Gribov¹⁴ in deriving the Reggeon diagram technique for 2-2

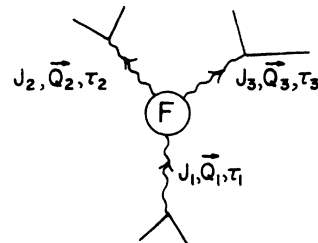


FIG. 3. The kinematic channels of the partial-wave amplitude for the six-point function. Each channel has angular momentum J_i , two-momentum \bar{Q}_i such that $|\bar{Q}_i|^2 = -t_i$, and signature $\tau_i = \pm 1$.

processes. This technique, which we adopt here, studies the high-energy, fixed-momentum-transfer behavior of hybrid field-theory graphs in which power behavior is attributed to internal two-to-two amplitudes when they carry large subenergies.⁴ The object of study is the signed partial-wave amplitude $F(J, t)$ from which the elastic amplitude $T(s, t)$ is gotten via

$$T(s, t) = \int_{c-i\infty}^{c+i\infty} \frac{dJ}{2\pi i} s^J \xi_J F(J, t), \quad (6)$$

with

$$\xi_J = \frac{e^{-i\pi J} + \tau}{\sin \pi J} \quad (7)$$

and $\tau = \pm 1$ is the signature. Gribov's Reggeon rules give a constructive procedure for evaluating the

$$T_{2 \rightarrow 3}(s, s_1, s_2, t_1, t_2) = \int \frac{dJ_1 dJ_2}{(2\pi i)^2} [s^{J_1} s_2^{J_2 - J_1} \xi_{J_1} \xi_{J_2 - J_1} F_1(J_1, J_2, t_1, t_2, \eta) + s^{J_2} s_1^{J_1 - J_2} \xi_{J_2} \xi_{J_1 - J_2} F_2(J_1, J_2, t_1, t_2, \eta)] , \quad (8)$$

where

$$\xi_{J_a - J_b} = \frac{e^{-i\pi(J_a - J_b)} + \tau_a \tau_b}{\sin \pi(J_a - J_b)}, \quad \eta = \frac{s}{s_1 s_2}, \quad (9)$$

and the signed partial-wave amplitudes F_i are real analytic. Reggeon rules yield the F_i .

Here we see one of the complicating features of inelastic s -channel amplitudes. The presence of two partial-wave amplitudes in (8) comes from the additional variables one requires to discuss the five-point function; in particular, the azimuthal angle or helicity variable. Two terms are also necessary to satisfy the so-called Steinmann relations which forbid simultaneous singularities in overlapping invariants. In (8) one may not allow a factor like $s_1^{J_1} s_2^{J_2}$, which seems so natural from the double-Regge picture of Fig. 4, since it has a simultaneous discontinuity in s_1 and s_2 . The combinations $s^{J_1} s_2^{J_2 - J_1}$ and $s^{J_2} s_1^{J_1 - J_2}$ are permitted, and the partial-wave decomposition of $T_{2 \rightarrow 3}$ contains both possibilities. For more complicated amplitudes, $T_{2 \rightarrow 4}$, etc., the number of allowed terms grows rapidly.

We see here, however, the clue how to begin. We must first identify the partial-wave amplitudes which are allowed by general principles and then find rules for evaluating Reggeon-cut contributions to them. We will proceed by considering the simplest hybrid graph that can contribute to the triple-Regge region. This is the triple-Regge pole graph in Fig. 5. In the study of $2 \rightarrow 3$ amplitudes

J -plane cut contributions to the real analytic function $F(J, t)$. These rules can be formulated in a field-theoretic fashion, and the solution of the problem thus stated by means of the renormalization group^{9,10} has provided substantial understanding of the detailed behavior of $F(J, t)$ near $J = 1, t = 0$ for the even-signed amplitude involving the P .

The derivation of Reggeon-cut rules for inelastic amplitudes is less well understood. In principle we would like to have as powerful an analytic tool as for the elastic amplitudes. For the multi-Regge regime of $2 \rightarrow N$ production amplitudes this instrument has been found.¹² For the $2 \rightarrow 3$ process, for example, one discovers that in the double-Regge limit (Fig. 4) one can write *pole and cut* contributions as

the structure that emerges from the simplest graph has the full content of Eq. (8). This will also be the case for us, so we give some detail of the procedure in our analysis of Fig. 5(b).

We are interested in studying the six-point amplitude T_6 for the scattering of spinless particles $p_1 + p_2 + p_3 \rightarrow p'_1 + p'_2 + p'_3$ in the triple-Regge limit. The contribution to T_6 we will analyze in detail is in Fig. 5. Each of the $2 \rightarrow 2$ subamplitudes will be required to have power behavior in its subenergy for fixed momentum transfers and finite off-shell masses. We will use the following (overcomplete) set of variables for T_6 (Fig. 1).

$$s_{12} = (p_1 + p_2)^2, \quad s_{13} = (p'_1 + p'_3)^2, \quad s_1 = (p_1 - Q_2)^2, \\ s_{23} = (p_3 - p'_2)^2, \quad s_2 = (p_2 + Q_1)^2, \quad s_3 = (p_3 - Q_2)^2, \quad (10)$$

and

$$t_i = Q_i^2 = (p_i - p'_i)^2, \quad i = 1, 2, 3.$$

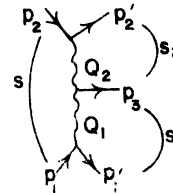


FIG. 4. The double-Regge region of the $2 \rightarrow 3$ amplitude.

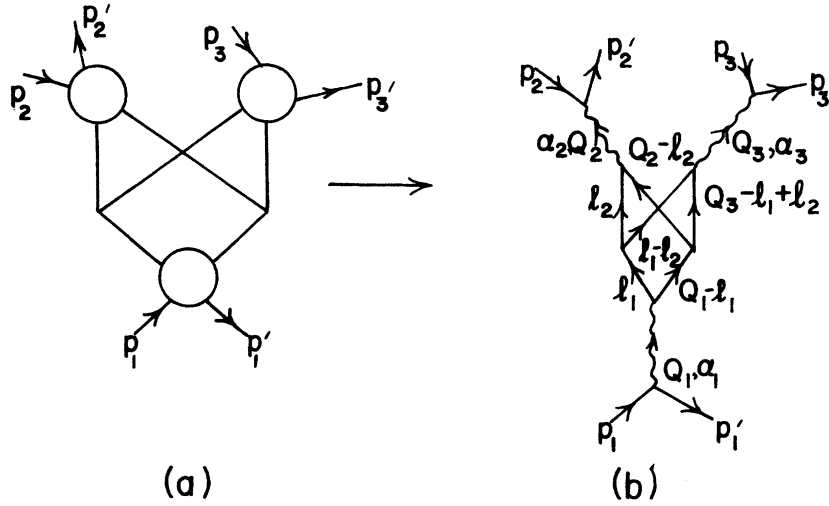


FIG. 5. The hybrid field-theory graph for the simplest contribution to T_6 in the triple-Regge region. Each of the $2 \rightarrow 2$ subamplitudes becomes a Reggeon when its subenergy is large. This is the transition from (a) to (b).

Since T_6 depends only on eight variables, one of these must be redundant. The requirement that T_6 be independent of the relative orientation angle of the planes between p_1 and p_1' , p_2 and p_2' , and p_3 and p_3' eliminates the extra variable via an unattractive nonlinear constraint on the variables in (10).^{15,16}

In the triple-Regge limit of T_6 we require

$$s_{12}, s_{13}, s_{11}, \frac{s_{12}}{s_1}, \frac{s_{13}}{s_1} \rightarrow \infty, \quad (11)$$

while

$$\frac{s_{13}}{s_{12}} \equiv R, \quad s_2, s_3, s_{23}, \text{ and the } t_i \quad (12)$$

are held fixed. To analyze Fig. 5(b) we decompose all vectors into their components along vectors \tilde{p}_1 and \tilde{p}_2 , which carry the "large" components of momenta, and along a remaining spacelike two-vector perpendicular to \tilde{p}_1 . These Sudakov¹⁷ variables allow us to carry out the integrations over the projections of loop momenta on the \tilde{p}_i , leaving the usual two-dimensional transverse dynamics to be specified. We define the "large" vectors \tilde{p}_i by

$$\tilde{p}_1 = p_1 - \frac{m^2}{s_{12}} p_2 \quad (13)$$

and

$$\tilde{p}_2 = p_3 - \frac{m^2}{s_{12}} p_1, \quad \text{where } p_1^2 = p_1'^2 = m^2. \quad (14)$$

Clearly \tilde{p}_1 lies "mostly" along p_1 , the "beam" direction, and \tilde{p}_2 lies mostly along p_2 . These vectors have the further virtue that to order $1/s_{12}$,

$\tilde{p}_1^2 = 0$, which means that in the evaluation of our hybrid graphs to order $1/s_{12}$, we may systematically drop \tilde{p}_1^2 . This order of error is quite adequate for us.

Now we wish to decompose all vectors as

$$v = A \tilde{p}_1 + B \tilde{p}_2 + v_{\perp}, \quad (15)$$

with

$$v_{\perp} \cdot \tilde{p}_1 = v_{\perp} \cdot \tilde{p}_2 = 0, \quad v_{\perp}^2 \leq 0. \quad (16)$$

The kinematic vectors \tilde{p}_i , \tilde{p}_i' , and Q_i are then

$$\tilde{p}_1 = \tilde{p}_1 + \frac{m^2}{s_{12}} \tilde{p}_2, \quad (17)$$

$$\tilde{p}_2 = \tilde{p}_2 + \frac{m^2}{s_{12}} \tilde{p}_1, \quad (18)$$

$$\tilde{p}_3 = \frac{m^2 - s_{23} - m^2 R + s_3 - t_2}{s_{12}} \tilde{p}_1 + R \tilde{p}_2 + \tilde{p}_{3\perp}, \quad (19)$$

$$Q_1 = \frac{s_2 - t_1 - m^2}{s_{12}} \tilde{p}_1 + \frac{t_1}{s_{12}} \tilde{p}_2 + Q_{1\perp}, \quad (20)$$

$$Q_2 = -\frac{t_2}{s_{12}} \tilde{p}_1 + \frac{m^2 + t_2 - s_1}{s_{12}} \tilde{p}_2 + Q_{2\perp}, \quad (21)$$

and

$$Q_3 = \frac{s_2 - m^2 + t_2 - t_1}{s_{12}} \tilde{p}_1 + \frac{s_1 - m^2 + t_1 - t_2}{s_{12}} \tilde{p}_2 + Q_{3\perp}. \quad (22)$$

The apparent asymmetry between vectors labeled "2" and those labeled "3" occurs because of our choice of basis vectors \tilde{p}_i . This asymmetry will disappear.

What we wish to do now is label the internal vec-

tors l_i by

$$l_i = A_i \tilde{p}_1 + B_i \tilde{p}_2 + l_{i\perp}, \quad i = 1, 2$$

and using

$$d^4 l_i = \frac{1}{2} |s_{12}| dA_i dB_i d^2 l_{i\perp} \quad (23)$$

carry out as much of the $dA_i dB_i$ integration as possible. Restrictions are put on the A_i and B_i by requiring that the energies across the Reggeons in Fig. 5(b) be large while insisting at the same time that the masses of all particle legs or momentum transfers be small, that is $\lesssim m^2$.

The Reggeon energies in our parametrization are as follows.

Reggeon with α_1 :

$$(p_1 - l_1)^2 = (1 - A_1) \left(\frac{m^2}{s_{12}} - B_1 \right) s_{12} + l_{1\perp}^2; \quad (24)$$

Reggeon with α_2 :

$$(p_2 + l_2)^2 = \left(\frac{m^2}{s_{12}} + A_2 \right) (1 + B_2) s_{12} + l_{2\perp}^2; \quad (25)$$

Reggeon with α_3 :

$$\begin{aligned} (p_3 + l_1 - l_2)^2 &= \left(A_1 - A_2 + \frac{m^2 - s_{23} - m^2 R + s_3 - t_2}{s_{12}} \right) \\ &\quad \times (R + B_1 - B_2) s_{12} \\ &\quad + (p_3 + l_1 - l_2)_{\perp}^2. \end{aligned} \quad (26)$$

The six denominators in this graph of Fig. 5(b) are

$$\begin{aligned} D_1 &= l_1^2 - m^2 + i\epsilon \\ &= A_1 B_1 s_{12} + l_{1\perp}^2 - m^2 + i\epsilon, \end{aligned} \quad (27)$$

$$\begin{aligned} D_2 &= (Q_1 - l_1)^2 - m^2 + i\epsilon \\ &= \left(\frac{s_2 - t_1 - m^2}{s_{12}} - A_1 \right) \left(\frac{t_1}{s_{12}} - B_1 \right) s_{12} \\ &\quad + (Q_1 - l_1)_{\perp}^2 - m^2 + i\epsilon, \end{aligned} \quad (28)$$

$$\begin{aligned} D_3 &= l_2^2 - m^2 + i\epsilon \\ &= A_2 B_2 s_{12} + l_{2\perp}^2 - m^2 + i\epsilon, \end{aligned} \quad (29)$$

$$\begin{aligned} D_4 &= (Q_3 - l_1 + l_2)^2 - m^2 + i\epsilon \\ &= \left(\frac{s_2 - m^2 + t_2 - t_1}{s_{12}} - A_1 + A_2 \right) \left(\frac{s_1}{s_{12}} - B_1 + B_2 \right) s_{12} \\ &\quad + (Q_3 - l_1 + l_2)_{\perp}^2 - m^2 + i\epsilon, \end{aligned} \quad (30)$$

$$\begin{aligned} D_5 &= (l_1 - l_2)^2 - m^2 + i\epsilon \\ &= (A_1 - A_2)(B_1 - B_2) s_{12} + (l_1 - l_2)_{\perp}^2 - m^2 + i\epsilon, \end{aligned} \quad (31)$$

and

$$\begin{aligned} D_6 &= (Q_2 - l_2)^2 - m^2 + i\epsilon \\ &= \left(-\frac{t_2}{s_{12}} - A_2 \right) \left(\frac{m^2 + t_2 - s_1}{s_{12}} - B_2 \right) s_{12} \\ &\quad + (Q_2 - l_2)_{\perp}^2 - m^2 + i\epsilon. \end{aligned} \quad (32)$$

We ask that each Reggeon energy be $\gg m^2$, and each $D_i \lesssim m^2$. This will give the most important contribution to T_6 from Fig. 5(b). The A_i and B_i are restricted then by

$$\frac{m^2}{s_{12}} \ll |A_2| \lesssim \frac{m^2}{s_1}, \quad (33)$$

$$|A_1| \lesssim \frac{m^2}{s_1}. \quad (34)$$

$$|B_2| \ll 1, \quad (35)$$

$$\frac{m^2}{s_{12}} \ll |B_1| \lesssim 1. \quad (36)$$

Also we require

$$l_{i\perp}^2 \lesssim m^2. \quad (37)$$

Using these conditions we may rewrite the Reggeon energies and the D_i as the following.

$$\text{energy for } \alpha_1: (p_1 - l_1)^2 \approx -B_1 s_{12}; \quad (38)$$

$$\text{energy for } \alpha_2: (p_2 + l_2)^2 \approx A_2 s_{12}; \quad (39)$$

and

$$\begin{aligned} \text{energy for } \alpha_3: (p_3 + l_1 - l_2)^2 &\approx (A_1 - A_2) R s_{12} \\ &= (A_1 - A_2) s_{13}; \end{aligned} \quad (40)$$

while

$$D_1 = A_1 B_1 s_{12} + l_{1\perp}^2 - m^2 + i\epsilon, \quad (41)$$

$$D_2 = A_1 B_1 s_{12} + (Q_1 - l_1)_{\perp}^2 - m^2 + i\epsilon, \quad (42)$$

$$D_3 = A_2 B_2 s_{12} + l_{2\perp}^2 - m^2 + i\epsilon, \quad (43)$$

$$\begin{aligned} D_4 &= (A_2 - A_1) \left(\frac{s_1}{s_{12}} - B_1 + B_2 \right) s_{12} \\ &\quad + (Q_3 - l_1 + l_2)_{\perp}^2 - m^2 + i\epsilon, \end{aligned} \quad (44)$$

$$D_5 = (A_1 - A_2)(B_1 - B_2) s_{12} + (l_1 - l_2)_{\perp}^2 - m^2 + i\epsilon, \quad (45)$$

$$D_6 = (A_2) \left(\frac{s_1}{s_{12}} + B_2 \right) s_{12} + (Q_2 - l_2)_{\perp}^2 - m^2 + i\epsilon. \quad (46)$$

In each of these expressions terms of order s_1/s_{12} have been retained while $O(m^2/s_{12})$ has been neglected.

Each Reggeon exchange carries a signature factor and enters T_6 as, for Reggeon 1, say,

$$\xi_{\alpha_1}(-B_1 s_{12})^{\alpha_1}, \tag{47}$$

using (38), where

$$\xi_{\alpha_1} = \frac{e^{-i\pi\alpha_1 + \tau_1}}{\sin\pi\alpha_1}. \tag{48}$$

If we call g the internal three-particle coupling constant and β the two-particle-Reggeon coupling, then with the high-energy approximations made so far we find for $T_6(\text{pole})$ [Fig. 5(b)]

$$T_6(\text{pole}) = \beta(t_1)\beta(t_2)\beta(t_3) \left[\frac{g}{(2\pi)^4} \right]^2 \frac{|s_{12}|^2}{4} \xi_{\alpha_1} \xi_{\alpha_2} \xi_{\alpha_3} (s_{12})^{\alpha_1 + \alpha_2} (s_{13})^{\alpha_3} \\ \times \int dA_1 dB_1 d^2 l_{1\perp} dA_2 dB_2 d^2 l_{2\perp} \frac{(-B_1)^{\alpha_1} (A_2)^{\alpha_2} (A_1 - A_2)^{\alpha_3} \beta^3}{D_1 \cdots D_6}. \tag{49}$$

The β 's under the integrals depend on the invariant masses of the particle legs in a complicated and uninteresting manner.

We wish to cast this integral into a form which explicitly exhibits the *energy dependence* and *phase structure*. From the form of the D_i we observe that the B_2 integration vanishes unless $\text{sgn} A_2 \neq \text{sgn}(A_2 - A_1)$, so either $0 \leq A_2 \leq A_1$ or $A_1 \leq A_2 \leq 0$. This allows us to split (49) into two parts using

$$\int dA_1 \int dA_2 = \int_0^\infty dA_1 \int_0^{A_1} dA_2 + \int_{-\infty}^0 dA_1 \int_{A_1}^0 dA_2. \tag{50}$$

Next noting that

$$\xi_{\alpha_1}(-B_1)^{\alpha_1} = \frac{(B_1 - i\epsilon)^{\alpha_1} + \tau_1(-B_1 - i\epsilon)^{\alpha_1}}{\sin\pi\alpha_1} \tag{51}$$

and

$$\xi_{\alpha_2}(A_2)^{\alpha_2} \xi_{\alpha_3}(A_1 - A_2)^{\alpha_3} = \tau_2 \tau_3 \xi_{\alpha_2} \xi_{\alpha_3} (-A_2)^{\alpha_2} (A_2 - A_1)^{\alpha_3}, \tag{52}$$

we may write $T_6(\text{pole})$ as

$$T_6(\text{pole}) = \text{const} \times s_{12}^{2+\alpha_1+\alpha_2} s_{13}^{\alpha_3} \xi_{\alpha_2} \xi_{\alpha_3} \\ \times \int d^2 l_{2\perp} d^2 l_{1\perp} \\ \times \int_{-\infty}^{+\infty} dB_2 dB_1 \left\{ \int_0^\infty dA_1 \int_0^{A_1} dA_2 \frac{(B_1 - i\epsilon)^{\alpha_1} + \tau_1(-B_1 - i\epsilon)^{\alpha_1}}{\sin\pi\alpha_1} (A_1 - A_2)^{\alpha_3} A_2^{\alpha_2} \right. \\ \left. + \tau_2 \tau_3 \int_{-\infty}^0 dA_1 \int_{A_1}^0 dA_2 \frac{(B_1 - i\epsilon)^{\alpha_1} + \tau_1(-B_1 - i\epsilon)^{\alpha_1}}{\sin\pi\alpha_1} (-A_2)^{\alpha_2} (A_2 - A_1)^{\alpha_3} \right\} \frac{\beta^3}{D_1 \cdots D_6}. \tag{53}$$

We turn our attention next to the B_1 integration. The singularities in B_1 are contained in the zeros of the D_i and in $(B_1 - i\epsilon)^{\alpha_1}$. The poles from the D_i are all in the lower half B_1 plane so we wrap the B_1 integration around the branch point at $B_1 = 0$ (see Fig. 6). Noting

$$\int_{-\infty}^{+\infty} dB_1 (B_1 - i\epsilon)^{\alpha_1} \frac{1}{D_1 \cdots D_6} = -2i \sin\pi\alpha_1 \int_{-\infty}^0 dB_1 \frac{(-B_1)^{\alpha_1}}{D_1 \cdots D_6}, \tag{54}$$

and a similar result for use in the second term of (53), we may write

$$T_6(\text{pole}) = s_{12}^{\alpha_2} s_{13}^{\alpha_3} \xi_{\alpha_2} \xi_{\alpha_3} [H(s_{12}, s_1) + \tau_1 \tau_2 \tau_3 H(s_{12}, -s_1)], \tag{55}$$

where

$$H(s_{12}, s_1) = -2i \times \text{const} \\ \times s_{12}^{2+\alpha_1} \int d^2 l_{1\perp} d^2 l_{2\perp} \int_{-\infty}^{+\infty} dB_2 \int_{-\infty}^0 dB_1 \int_0^\infty dA_1 \int_0^{A_1} dA_2 (A_2)^{\alpha_2} (A_1 - A_2)^{\alpha_3} (-B_1)^{\alpha_1} \frac{\beta^3}{D_1 \cdots D_6}. \tag{56}$$

To proceed we scale out the s_{12} dependence of $H(s_{12}, s_1)$ by the change of variables $A_2 = \chi A_1$, $\tilde{B}_2 = s_{12} B_2$, $\tilde{B}_1 = s_{12} B_1$, so

$$H(s_{12}, s_1) = -2i \times \text{const} \times \int d^2 l_{1\perp} d^2 l_{2\perp} \int_{-\infty}^{+\infty} d\tilde{B}_2 \int_{-\infty}^0 d\tilde{B}_1 \int_0^{\infty} dA_1 \int_0^1 d\chi (-\tilde{B}_1)^{\alpha_1} (A_1)^{\alpha_2 + \alpha_3 + 1} \chi^{\alpha_2} (1 - \chi)^{\alpha_3} \frac{\beta^3}{D_1 \cdots D_6}. \tag{57}$$

This function H has a right-hand cut due to a pinch in the denominators D_5 and D_6 and a left-hand cut from pinching of zeros in D_3 and D_4 . This observation makes it easy to evaluate $\text{disc}_{s_1} H(s_{12}, s_1)$ on the right-hand cut,

$$\frac{\text{disc}_{s_1} H(s_{12}, s_1)}{2i} \Bigg|_{s_1 > 0} = \left[\frac{g}{(2\pi)^4} \right]^2 \frac{\beta(t_1)\beta(t_2)\beta(t_3)}{4} (2\pi)^2 s_1^{\alpha_1 - \alpha_2 - \alpha_3} \times \int d^2 l_{1\perp} d^2 l_{2\perp} \int_{-\infty}^0 dB'_1 \int_0^{\infty} dA'_1 \int_0^1 d\chi (-B'_1)^{\alpha_1} (A'_1)^{\alpha_2 + \alpha_3} \chi^{\alpha_2 - 1} (1 - \chi)^{\alpha_3} \frac{\beta^3}{D_1 \cdots D_4} \delta(D_5), \tag{58}$$

where we have let $A'_1 = s_1 A_1$, $B'_1 = \tilde{B}_1 / s_1$, and the \tilde{B}_2 integral has been evaluated using $\delta(D_6)$. Now we have $\text{disc}_{s_1} H(s_{12}, s_1) / 2i$ for large s_1 as $(s_1)^{\text{power}}$ times a real, positive function. Thus we learn¹⁸

$$H(s_{12}, s_1) + \tau_1 \tau_2 \tau_3 H(s_{12}, -s_1) = - (s_1)^{\alpha_1 - \alpha_2 - \alpha_3} \xi_{\alpha_1 - \alpha_2 - \alpha_3} r_{\alpha_1, \alpha_2, \alpha_3} \beta(t_1)\beta(t_2)\beta(t_3), \tag{59}$$

where $r_{\alpha_1, \alpha_2, \alpha_3}$ is a real integral over the $A_i, B_i, l_{i\perp}$. Now we have for T_6 (pole)

$$T_6(\text{pole}) = - \beta(t_1)\beta(t_2)\beta(t_3) s_{12}^{\alpha_2} \xi_{\alpha_2} s_{13}^{\alpha_3} \xi_{\alpha_3} s_1^{\alpha_1 - \alpha_2 - \alpha_3} \xi_{\alpha_1 - \alpha_2 - \alpha_3} r_{\alpha_1, \alpha_2, \alpha_3}. \tag{60}$$

For application to the inclusive process we must replace ξ_{α_3} by $\xi_{\alpha_3}^*$.

This is the form we have been reaching for. All phases of T_6 in the triple-Regge region are contained in the signature factors.¹⁹ The coefficient (beside the two-particle-Reggeon couplings β) is a real triple-Reggeon coupling. If we write

$$T_6(\text{pole}) = - \int \frac{dJ_1 \cdots dJ_3}{(2\pi i)^3} s_{12}^{J_2} \xi_{J_2} s_{13}^{J_3} \xi_{J_3} s_1^{J_1 - J_2 - J_3} \xi_{J_1 - J_2 - J_3} F(J_1, J_2, J_3, t_1, t_2, t_3), \tag{61}$$

then (60) results from a triple pole in F with factorized residue

$$F_{\text{pole}}(J_1, J_2, J_3, t_1, t_2, t_3) = \frac{\beta(t_1)\beta(t_2)\beta(t_3) r_{J_1, J_2, J_3}}{[J_1 - \alpha_1(t_1)] \cdots [J_3 - \alpha_3(t_3)]}. \tag{62}$$

We might conjecture, and will soon show, that precisely (61) emerges from more complicated Reggeon graphs involving branch points as well as poles; only $F(J_i, t_i)$ will be altered.

Two observations will close this section. First, our triple-Reggeon coupling reduces to the one found by Gribov¹⁴ in his study of diagrams for the elastic amplitude when $1 - \alpha_1(t_1) = 1 - \alpha_2(t_2) + 1 - \alpha_3(t_3)$. The quantity $1 - \alpha_i$ plays the role of a conserved "energy" in Reggeon field theories^{4, 9, 10} and so our r may be interpreted as the "off-energy-shell" triple-Reggeon vertex. Such an off-shell quantity plays a key role in the triple-Regge region as we can see by the observation that, in

general, $1 - J_1 \neq 1 - J_2 + 1 - J_3$ for the triple-partial-wave amplitude involved in T_6 . This energy "non-conservation" goes away when we join p'_2 and p_3 to determine the triple-Regge contribution to T_{elastic} (Fig. 7).

Second, in the limit $s_{12} = s_{13} = s$, $t_2 = t_3 = t$, $t_1 = 0$ this graph of Fig. 5(b) has been evaluated by Mueller and Trueman.²⁰ Our agreement with the general partial-wave analysis of Ref. 15 and the arguments of Ref. 19 gives us some confidence in our answer.

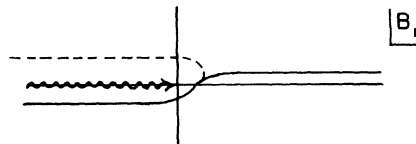


FIG. 6. The complex B_1 plane needed in the evaluation of the graph in Fig. 5.

III. GENERAL ANALYTIC STRUCTURE OF T_6

Before we launch into a discussion of more complicated hybrid diagrams we pause to make further comment on Eq. (60). This does not contain the full structure allowed to T_6 in the triple-Regge limit. In requiring the energy across each Reggeon in our graph to be large ($\gg m^2$), we have picked up only those contributions which have a nonzero discontinuity in s_1 . This is sufficient for our present task, but for a fuller understanding it is worthwhile to see what we have omitted.

For the allowed structure of T_6 we use some results from the literature.²¹ Start with the genuine

$$\begin{aligned}
 T_6(\text{pole}) = & \beta(t_1)\beta(t_2)\beta(t_3) \left[\xi_{\alpha_2} \xi_{\alpha_3} \xi_{\alpha_1 - \alpha_2 - \alpha_3} s_1^{\alpha_1 - \alpha_2 - \alpha_3} s_{12}^{\alpha_2} s_{13}^{\alpha_3} V_{23} \right. \\
 & + \xi_{\alpha_1} \xi_{\alpha_2} \xi_{\alpha_3 - \alpha_1 - \alpha_2} s_3^{\alpha_3 - \alpha_1 - \alpha_2} s_{23}^{\alpha_2} s_{13}^{\alpha_1} V_{12} + \xi_{\alpha_1} \xi_{\alpha_3} \xi_{\alpha_2 - \alpha_1 - \alpha_3} s_2^{\alpha_2 - \alpha_1 - \alpha_3} s_{12}^{\alpha_1} s_{23}^{\alpha_3} V_{13} \\
 & + e^{-i\pi(\alpha_1 + \alpha_2 + \alpha_3)/2} (1 + \tau_1 e^{i\pi\alpha_1} + \tau_2 e^{i\pi\alpha_2} + \tau_3 e^{i\pi\alpha_3}) \\
 & \left. \times s_{12}^{(\alpha_1 + \alpha_2 - \alpha_3)/2} s_{13}^{(\alpha_1 + \alpha_3 - \alpha_2)/2} s_{23}^{(\alpha_2 + \alpha_3 - \alpha_1)/2} V_{123} \right], \quad (63)
 \end{aligned}$$

where the V 's are real analytic functions of the t_i and $\eta_{ij} = s_{ij}/s_i s_j$. These four terms correspond to the four allowed combinations of simultaneous discontinuities of T_6 as illustrated in Fig. 8.

The fourth term deserves further comment. The derivation of (63) proceeds via a triple-partial-wave expansion and Sommerfeld-Watson transform of T_6 , leading to

$$s_1^{\alpha_1} s_2^{\alpha_2} s_3^{\alpha_3} W(\eta_{ij}, t_i). \quad (64)$$

Then the function W is expanded about $\eta_{ij}^{-1} = 0$, and the V 's are expressed as power series in η_{ij}^{-1} regular at $\eta_{ij}^{-1} = 0$. For the physical amplitude the η_{ij} are not independent, therefore they cannot be taken independently large but one must observe the constraint

$$\eta_{ij} \sim \eta_{ik} \eta_{kj}. \quad (65)$$

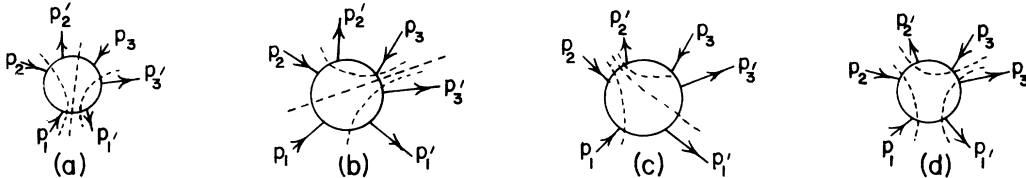


FIG. 8. The allowed simultaneous energy discontinuities of T_6 . The dashed lines denote the subenergies in which the amplitude has nonvanishing discontinuities. Intersecting lines correspond to cuts in overlapping channels. Only (a) has a discontinuity in s_1 and contributes to the inclusive process of Fig. 2.

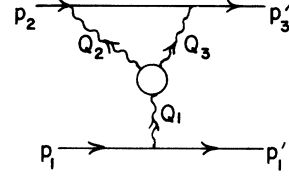


FIG. 7. The triple-Regge contribution to T_{elastic} . When s_1 is integrated over in Fig. 5, energy is conserved and the vertex γ in Fig. 5 becomes the usual triple-Regge vertex of Ref. 4 or Ref. 14.

triple-Regge limit $s_i \rightarrow \infty$; that is, the crossed cosines of angles conjugate to J_i becoming large. In Ref. 21 it is argued that when the $s_i \rightarrow \infty$, T_6 (pole) has the form

For example, take $\eta_{13} \sim \eta_{12} \eta_{23}$, then the fourth term in (63) becomes

$$s_2^{\alpha_2 - \alpha_1 - \alpha_3} s_{12}^{\alpha_1} s_{23}^{\alpha_3} (\text{phase factor}) V_{123}, \quad (66)$$

which has an identical *energy dependence* to the third term of (63). The *phase structure* is quite different.

Until now we have been talking about the triple-Regge limit $s_i \rightarrow \infty$. In the mixed limit we take on T_6 to get the inclusive cross section^{15,21}; we still expect a sum of four possible terms having the same structure as (63). This is because the singularities in complex helicity needed for the mixed limit are tied to the J_i singularities.^{15,16} However, since s_2 and s_3 remain finite the corresponding angular momentum integrals cannot be opened up except in the first term. We, then, have

$$T_6 = -\beta(t_1) \left[\xi_{\alpha_2} \xi_{\alpha_3} \xi_{\alpha_1 - \alpha_2 - \alpha_3} s_1^{\alpha_1 - \alpha_2 - \alpha_3} s_{12}^{\alpha_2} s_{13}^{\alpha_3} g(\alpha_1, \alpha_2, \alpha_3, t_i) \beta(t_1) \beta(t_2) \right. \\ \left. + \int dJ_2 dJ_3 \xi_{\alpha_1} \xi_{J_2} \xi_{J_3 - \alpha_1 - J_2} s_{13}^{\alpha_1} s_{23}^{J_2} s_3^{J_3 - \alpha_1 - J_2} F_{12}(\alpha_1, J_2, J_3, t_i) + \text{two other terms} \right], \quad (67)$$

and no dependence on η_{23} appears in the first term. The fourth term contributes no discontinuity in s_1 .

What we wish to emphasize in all this is that T_6 has four independent partial-wave amplitudes, but only one yields a discontinuity in s_1 , the missing mass. It is this term that our hybrid graph analysis has yielded. The remaining terms differ from this in that they do not expose the leading J -plane singularity in the t_2 or t_3 channels. This makes it quite plausible that in our analysis of the hybrid diagrams, they will be absent. This is consistent with the observations in Ref. 20.

We close this section with another salient observation about (67). The signature factors of the first term show that it has particle poles in t_2 and t_3 . It may be viewed as a contribution to the amplitude for particle 1 + Reggeon α_2 - particle 1' + Reggeon α_3 (Fig. 9). Such an amplitude will have many features in common with 2-2 particle amplitudes. One of these is the Gribov-Pomeranchuk fixed pole at nonsense values of J_1 , the angular momentum in the t_1 channel. In our amplitude this is in the signature factor $\xi_{\alpha_1 - \alpha_2 - \alpha_3}$ and occurs at

$\alpha_1 = \alpha_2 + \alpha_3 - 1$. The residue of this pole is exactly what appears as the triple-Reggeon vertex in Gribov's diagram technique for the elastic amplitudes. This explains why our $r_{\alpha_1, \alpha_2, \alpha_3}$ must agree with Gribov's at this nonsense point. It also explains why we took the *nonplanar* hybrid graph in Fig. 5 rather than its simpler planar brother. The latter will be missing the needed fixed pole.²⁰

IV. DIAGRAMS WITH BRANCH POINTS IN J

We turn our attention now to more elaborate hybrid graphs which will give J -plane cuts in the triple-Regge partial-wave amplitude. Our task will be to examine several configurations of graphs and find the phase and energy variation exhibited in Eq. (61).

Our first hybrid graph is shown in Fig. 10. Our aim is to identify various blocks of this graph as known parts from previous analyses; for example, $r_{\alpha_a, \alpha_b, \alpha_c}$ from Sec. II and the two Reggeon-two particle function N_2 from elastic amplitude studies.^{4, 14} The expression for the present graph is

$$T_6 = -i \int \frac{d^4 k}{(2\pi)^4} g^2 \int \frac{d^4 k_1}{(2\pi)^4} \frac{\beta^2}{D_1 \cdots D_4} g^2 \int \frac{d^4 k_2}{(2\pi)^4} \frac{\beta^2}{D_5 \cdots D_8} \\ \times g^2 \int \frac{d^4 l_1 d^4 l_2}{(2\pi)^8} \frac{\beta^3}{D_9 \cdots D_{14}} \xi_{\alpha_1} [(p_1 - k_1 - l_1)^2]^{\alpha_1} \xi_{\alpha_2} [(p_2 + l_2 - k_2)^2]^{\alpha_2} \\ \times \xi_{\alpha_3} [(p_3 + l_1 - l_2)^2]^{\alpha_3} \xi_{\alpha_4} [(k_1 + k_2)^2]^{\alpha_4}, \quad (68)$$

where

$$\alpha_1 = \alpha [(Q_1 + k)^2], \quad (69)$$

$$\alpha_2 = \alpha [(Q_2 + k)^2], \quad (70)$$

$$\alpha_3 = \alpha [Q_3^2], \quad (71)$$

and

$$\alpha_4 = \alpha [k^2]. \quad (72)$$

We use the same set of parameters as before:

$$k = a\tilde{p}_1 + b\tilde{p}_2 + k_{\perp}, \quad (73)$$

$$k_i = a_i\tilde{p}_1 + b_i\tilde{p}_2 + k_{i\perp}, \quad i = 1, 2 \quad (74)$$

and

$$l_i = A_i\tilde{p}_1 + B_i\tilde{p}_2 + l_{i\perp}, \quad i = 1, 2. \quad (75)$$

Next we examine each D_i and ask that it be finite; i.e., $D_i \lesssim m^2$. For the lower vertex in Fig. 10(b) this means

$$k_{\perp}^2 = a_1 b_1 s_{12} + k_{1\perp}^2 \lesssim m^2, \quad (76)$$

$$(p_1 - k_1)^2 = (1 - a_1) b_1 s_{12} + k_{1\perp}^2 \lesssim m^2, \quad \text{etc.} \quad (77)$$

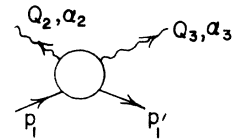


FIG. 9. The two-Reggeon-two-particle amplitude.

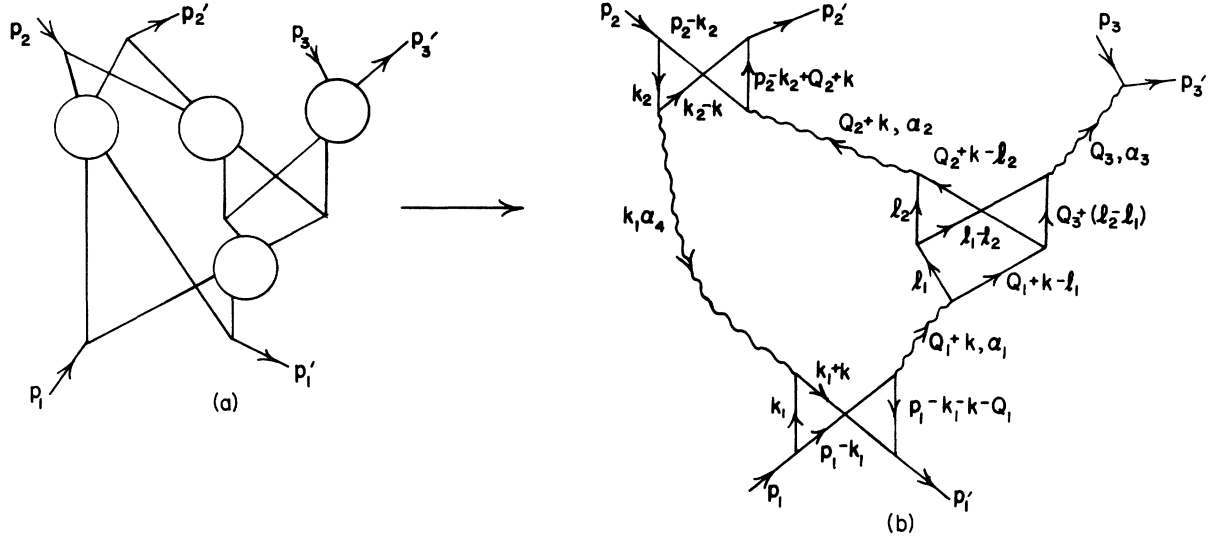


FIG. 10. A hybrid field-theory graph (a) and its Reggeon limit (b) which contains J -plane branch points.

from which we learn

$$|b_1| \lesssim \frac{m^2}{s_{12}}, \quad |b| \lesssim \frac{m^2}{s_{12}},$$

$$|a_1| \lesssim 1, \quad |a| \lesssim 1, \quad (78)$$

$$k_{1\perp}^2 \lesssim m^2.$$

The same restriction on the upper-left vertex shows us

$$|a_2| \lesssim \frac{m^2}{s_{12}}, \quad |a| \lesssim \frac{m^2}{s_{12}},$$

$$|b_2| \lesssim 1, \quad |b| \lesssim 1, \quad (79)$$

$$k_{2\perp}^2 \lesssim m^2,$$

and together these require

$$|a| \lesssim m^2/s_{12}, \quad |b| \lesssim m^2/s_{12}. \quad (80)$$

All these conditions have an elementary interpretation. Any vector with $a \lesssim 1$, $b \lesssim m^2/s_{12}$ lies primarily along p_1 and its inner product with any vector with $b \lesssim 1$, $a \lesssim m^2/s_{12}$ will be large of order abs_{12} . The subenergies in the lower blob are finite so the vectors there must have very small b_i since p_1 enters there and has $a = 1$. The same goes for the vectors in the upper left of Fig. 10(b): They must have very small a_i since p_2 with $b = 1$ enters. Since k connects the two blobs, both a and b for it must be small. It can carry transverse momentum only.

We also require that each Reggeon carry energy $\gg m^2$; this means the following.

Reggeon with α_1 :

$$(p_1 - k_1 - l_1)^2 \approx (1 - a_1)(-B_1)s_{12}; \quad (81)$$

Reggeon with α_2 :

$$(p_2 + l_2 - k_2)^2 \approx A_2(1 - b_2)s_{12}; \quad (82)$$

Reggeon with α_3 :

$$(p_3 + l_1 - l_2)^2 \approx (A_1 - A_2)s_{13}; \quad (83)$$

and

Reggeon with α_4 :

$$(k_1 + k_2)^2 \approx a_1 b_2 s_{12}. \quad (84)$$

In writing this we have incorporated the requirements that the denominators $D_9 \cdots D_{14}$ in the central vertex be $\lesssim m^2$. These Reggeon energies are large only if

$$\frac{m^2}{s_{12}} \ll |a_1|, |b_2|, |B_1|, |A_2|, \text{ and } |A_1 - A_2|. \quad (85)$$

Now we use these statements about the sizes of the a and b parameters to examine the components of Fig. 10(b). First look at the lower cross; its denominators are

$$D_1 = k_1^2 - m^2 + i\epsilon \\ = s_{12} a_1 b_1 + k_{1\perp}^2 - m^2 + i\epsilon, \quad (86)$$

$$D_2 = (p_1 - k_1)^2 - m^2 + i\epsilon \\ = (1 - a_1) \left(\frac{m^2}{s_{12}} - b_1 \right) s_{12} + k_{1\perp}^2 - m^2 + i\epsilon, \quad (87)$$

$$D_3 = (k_1 + k)^2 - m^2 + i\epsilon \\ = a_1 (b_1 + b) s_{12} + (k_1 + k)_{\perp}^2 - m^2 + i\epsilon, \quad (88)$$

and

$$\begin{aligned} D_4 &= (p_1 - k_1 - k - Q_1)^2 - m^2 + i\epsilon \\ &= (1 - a_1) \left(\frac{m^2}{s_{12}} - b_1 - b - \frac{t_1}{s_{12}} \right) s_{12} \\ &\quad + (k_1 + k + Q_1)_\perp^2 - m^2 + i\epsilon. \end{aligned} \quad (89)$$

The parameter a does not appear here since it is

much smaller [$O(m^2/s_{12})$] than a_1 . So the lower vertex has no dependence on a . Similarly the upper-cross denominators $D_5 \cdots D_8$ have no dependence on b . Furthermore, the central triple-Reggeon vertex depends on neither a nor b and has precisely the form we derived above for $r_{\alpha_1, \alpha_2, \alpha_3}$.

Thus we may collect together the integrations of the central vertex as

$$\begin{aligned} \xi_{\alpha_1} \xi_{\alpha_2} \xi_{\alpha_3} s_{12}^{\alpha_1 + \alpha_2} s_{13}^{\alpha_3} \frac{g^2 |s_{12}|^2}{4(2\pi)^8} \int \frac{dA_1 dB_1 d^2 l_{1\perp} dA_2 dB_2 d^2 l_{2\perp} \beta^3}{D_9 \cdots D_{14}} (-B_1)^{\alpha_1} A_2^{\alpha_2} (A_1 - A_2)^{\alpha_3} \\ = -\xi_{\alpha_2} \xi_{\alpha_3} \xi_{\alpha_1 - \alpha_2 - \alpha_3} s_{12}^{\alpha_2} s_{13}^{\alpha_3} s_1^{\alpha_1 - \alpha_2 - \alpha_3} r_{\alpha_1, \alpha_2, \alpha_3}, \end{aligned} \quad (90)$$

using the analysis of Sec. II. We move the b integration in Eq. (68) down to the lower vertex and note

$$\frac{g^2 |s_{12}|}{2(2\pi)^4} \int db \int \frac{da_1 db_1 d^2 k_{1\perp} (1 - a_1)^{\alpha_1} a_1^{\alpha_4} \beta^2}{D_1 \cdots D_4} = N_{\alpha_1 \alpha_4} \frac{\sqrt{2} 2\pi}{|s_{12}|}, \quad (91)$$

where N_{α_1, α_4} is the standard two-Reggeon-two-particle amplitude one encounters in the elastic-amplitude diagram analysis; it is real and independent of s_{12} . Doing the same on the upper vertex we find an $N_{\alpha_2 \alpha_4}$, then we write

$$T_6(\text{Fig. 10(b)}) = \frac{i}{4} \int \frac{d^2 k_{1\perp}}{(2\pi)^2} N_{\alpha_1 \alpha_4} N_{\alpha_2 \alpha_4} r_{\alpha_1, \alpha_2, \alpha_3} s_{12}^{\alpha_2 + \alpha_4 - 1} s_{13}^{\alpha_3} s_1^{\alpha_1 - \alpha_2 - \alpha_3} \xi_{\alpha_3} \xi_{\alpha_1 - \alpha_2 - \alpha_3} (\xi_{\alpha_2} \xi_{\alpha_4}). \quad (92)$$

In this combine ξ_{α_2} and ξ_{α_4} via

$$\xi_{\alpha_2} \xi_{\alpha_4} = i \gamma_{\alpha_2 \alpha_4} \xi_{\alpha_2 + \alpha_4 - 1}, \quad (93)$$

where

$$\gamma_{\alpha_2 \alpha_4} = \frac{\cos \frac{1}{2} \pi (\alpha_2 + \alpha_4 + 1 - \frac{1}{2} (\tau_2 + \tau_4))}{\sin \frac{1}{2} \pi (\alpha_2 + \frac{1}{2} (1 - \tau_2)) \sin \frac{1}{2} \pi (\alpha_4 + \frac{1}{2} (1 - \tau_4))}, \quad (94)$$

and

$$\xi_{\alpha_2 + \alpha_4 - 1} = \frac{e^{-i\pi(\alpha_2 + \alpha_4 - 1)} + \tau_2 \tau_4}{\sin \pi (\alpha_2 + \alpha_4 - 1)}. \quad (95)$$

Noting that the signatured partial-wave amplitude

$F(J_i, t_i)$ is

$$F(J_i, t_i) = \int ds_1 s_1^{-J_1 - 1} \int d \left(\frac{s_{12}}{s_1} \right) \left(\frac{s_{12}}{s_1} \right)^{-J_2 - 1} \int d \left(\frac{s_{13}}{s_1} \right) \left(\frac{s_{13}}{s_1} \right)^{-J_3 - 1} \frac{1}{(2i)^3} \text{disc}_{s_1} \text{disc}_{s_{12}} \text{disc}_{s_{13}} T_6, \quad (96)$$

we have

$$\begin{aligned} F(\text{Fig. 10(b)}) &= \int \frac{d^2 k_{1\perp}}{(2\pi)^2} \int \frac{dl_1 \cdots dl_4}{(2\pi i)^4} N_{l_1 l_4} N_{l_2 l_4} r_{l_1, l_2, l_3} \gamma_{l_2 l_4} G_{l_1}(\alpha_1) G_{l_2}(\alpha_2) G_{l_3}(\alpha_3) G_{l_4}(\alpha_4) \\ &\quad \times \frac{1}{[J_1 - (l_1 + l_4 - 1)][J_2 - (l_2 + l_4 - 1)][J_3 - l_3]} \end{aligned} \quad (97)$$

in which we have introduced a Mellin transform for each Reggeon,

$$s^\alpha \xi_\alpha = \int \frac{dl}{2\pi i} \xi_l s^l G_l(\alpha), \quad (98)$$

and

$$G_{l_1}(\alpha_i) = \frac{1}{l - \alpha_i (q_{i\perp}^2)} \quad (99)$$

for a Reggeon carrying momentum $q_{i\perp}$.

This shows that our amplitude can be represented in the form advertised, Eq. (4), and that the partial-

wave amplitude is real analytic. Noting that in (97) the l_i integrations lie to the right of the poles in G_{l_i} and the J_i contours in recovering T_6 lie to the right of J singularities, we write (97) as

$$\begin{aligned}
 F(J_i, t_i) = & \int \frac{d^2 k_{\perp}}{(2\pi)^2} \frac{d^2 k_{1\perp}}{(2\pi)^2} \frac{d^2 k_{2\perp}}{(2\pi)^2} \int \frac{dl_1 dl_2 dl_4}{(2\pi i)^3} (2\pi)^2 \delta^2(Q_{1\perp} - k_{1\perp} + k_{\perp}) (2\pi)^2 \delta^2(Q_{2\perp} + k_{\perp} - k_{2\perp}) \\
 & \times (2\pi i) \delta(J_1 - (l_1 + l_4 - 1)) 2\pi i \delta(J_2 - (l_2 + l_4 - 1)) \\
 & \times N_{l_1 l_4} N_{l_2 l_4} \gamma_{l_2 l_4} \gamma_{l_1 l_2} \gamma_{l_1 l_4} G_{l_1}(\alpha_1(k_{1\perp}^2)) G_{l_2}(\alpha_2(k_{2\perp}^2)) G_{l_4}(\alpha_4(k_{\perp}^2)) G_{J_3}(\alpha_3(Q_{3\perp}^2)).
 \end{aligned} \tag{100}$$

This formula has the following content:

(a) Each Reggeon line carries a two-momentum and an angular momentum and has a propagator $G_l(k_{\perp}^2) = [l - \alpha(k_{\perp}^2)]^{-1}$. Each Reggeon line is directed "upward" in the sense of increasing rapidity.

(b) At each vertex two-momentum is conserved.

(c) $1 - l$ is conserved everywhere except at the triple-Reggeon vertex.

(d) Each loop l_i and $k_{i\perp}$ is integrated over.

(e) The upper-left vertex carries a $\gamma_{l_2 l_4}$. At physical J_2 , $\gamma_{l_2 l_4}$ is zero and decouples the cut from physical partial waves.

To Fig. 10(b) then we can associate the Reggeon graph of Fig. 11. Note the direction of the Reggeon lines.

The vertex $N_{\alpha_1 \alpha_2}$ is the same as encountered in the Reggeon graphs for the elastic amplitudes. This identity holds for generalizations of the sim-

$$\beta(t_1) \beta(t_2) \beta(t_3) G_{J_1}(t_1) G_{J_2}(t_2) G_{J_3}(t_3) \bar{\Gamma}(J_i, t_i),$$

with

$$\begin{aligned}
 \bar{\Gamma}(J_i, t_i) = & \int \frac{d^2 k_{\perp}}{(2\pi)^2} \int \frac{dl_1 dl_2 dl_4}{(2\pi i)^3} (2\pi i) \delta(J_1 - (l_1 + l_4 - 1)) (2\pi i) \delta(J_2 - (l_2 + l_4 - 1)) \\
 & \times \gamma_{J_1 l_1 l_4} \gamma_{J_2 l_2 l_4} \gamma_{l_2 l_4} G_{l_1} G_{l_2} G_{l_4} \gamma_{l_1 l_2} \gamma_{l_1 l_4}.
 \end{aligned} \tag{103}$$

It is thus not difficult to find the partial-wave amplitude for Fig. 13(a) or Fig. 13(b): Taking for the central loop the expression (103), we can treat these diagrams in the same way as Fig. 11, where we had γ instead of $\bar{\Gamma}$.

Thus our rules allow us already to find the expressions for quite a large class of diagrams. As to the question of the energy ($1 - l$) nonconserving vertex, there is exactly one in each of these diagrams, and we can describe its location in the following way:

If we enter the Reggeon diagram at the bottom and move upwards toward the two upper ends, then at some stage this diagram splits into two

ple cross used in Fig. 10. In particular for the graph of Fig. 12 we note that the substitutions

$$N_{l_2 l_4}(k_{2\perp}, Q_{2\perp} - k_{2\perp}) \rightarrow \beta(Q_{2\perp}^2) G_{J_2}(\alpha(Q_{2\perp}^2)) \gamma_{J_2 l_2 l_4}, \tag{101}$$

and

$$N_{l_1 l_4}(k_{1\perp}, Q_{1\perp} - k_{1\perp}) \rightarrow \beta(Q_{1\perp}^2) G_{J_1}(\alpha(Q_{1\perp}^2)) \gamma_{J_1 l_1 l_4}, \tag{102}$$

yields the partial-wave amplitude. Since Reggeon energy, $1 - l$, is conserved in the γ 's of (101) and (102), these are the familiar Reggeon vertices.^{4,14}

The next observation we make is that Fig. 12 has the same structure as the triple-pole diagram of Fig. 5(b), when the central part is considered as a "radiative correction" to the triple-Reggeon vertex. This structure is also found in the form of the partial wave F of Fig. 12:

branches which then lead to the two separated upper ends. In all diagrams we have considered so far we can locate a vertex which represents the "last" interaction between the two branches; above this vertex there is no further interaction between

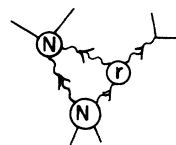


FIG. 11. The Reggeon graph corresponding to Fig. 10. Energy is not conserved at the vertex γ .

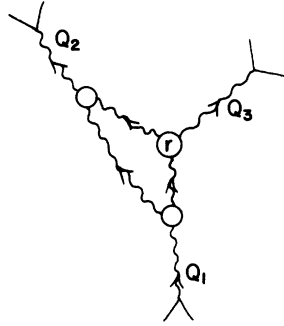


FIG. 12. A Reggeon graph with only single-Reggeon connections to the external particles. It is otherwise like Fig. 11. Energy is not conserved only at the vertex labeled with an r .

Reggeons of the different branches. It is this vertex where Reggeon energy is not conserved. If we now add to the rules above this general definition of the energy-nonconserving vertex, then our set of rules describes all our diagrams.

Finally, we want to note an important feature. If the external Reggeon energies $E_i = 1 - J_i$ are chosen so that

$$E_1 = E_2 + E_3, \quad (104)$$

then total energy is conserved. Since all vertices except for one do conserve energy, the over-all conservation propagates through the diagram, and the energies at the nonconserving vertex are forced onto the energy-conservation shell. At this point, as we have mentioned, the energies nonconserving vertex $r_{\alpha_1, \alpha_2, \alpha_3}$ equals the conserving vertex. Consequently, Γ obeys the same rules as the triple-Reggeon vertex function of the elastic Reggeon calculus.

V. THE DOUBLE CROSSED GRAPH

In the hybrid graphs we have considered until now it has been straightforward to identify at which vertex Reggeon energy is not conserved. The rule of the "last" interaction from the J_1 channel before the graph splits into the J_2 and J_3 channels suffices. That there remains a problem is seen by the Reggeon graph of Fig. 14(a): Should energy not be conserved at vertex A or vertex B? To answer this we return to our hybrid graphs, now considering Fig. 14(b).

Parametrize all the internal four-vectors as

$$k_i = a_i \tilde{p}_1 + b_i \tilde{p}_2 + k_{i\perp}, \quad i = 1, \dots, 5 \quad (105)$$

$$l_i = A_i \tilde{p}_1 + B_i \tilde{p}_2 + l_{i\perp}, \quad i = 1, \dots, 4. \quad (106)$$

First we show that this amplitude has the form of three N vertices and two r vertices which are connected by two-dimensional integrations over $k_{1\perp}$

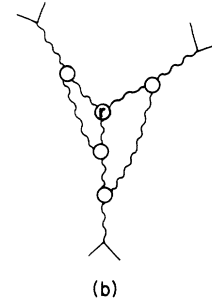
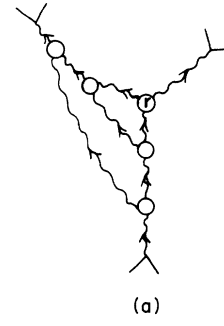


FIG. 13. Other Reggeon graphs. Energy is not conserved only at the vertex labeled with an r . These and the graphs of Figs. 12, 11, and 5 have only one branching vertex (see text).

and $k_{2\perp}$. So we begin by requiring all the denominators in the lower and upper right and left vertices to be $\lesssim m^2$. This yields

$$|a_3| \lesssim 1, \quad |b_3| \lesssim m^2/s_{12}, \quad k_{3\perp}^2 \lesssim m^2, \quad (107)$$

$$|b_4| \lesssim 1, \quad |a_4| \lesssim m^2/s_{12}, \quad k_{4\perp}^2 \lesssim m^2, \quad (108)$$

$$|b_5| \lesssim 1, \quad |a_5| \lesssim m^2/s_{12}, \quad k_{5\perp}^2 \lesssim m^2, \quad (109)$$

which is expected since k_3 is associated with p_1 through no large energies and k_4 and k_5 carry momentum mostly along p_2 . The restrictions on k_1 and k_2 yield

$$|a_1| \lesssim m^2/s_{12}, \quad |b_1| \lesssim m^2/s_{12}, \quad k_{1\perp}^2 \lesssim m^2, \quad (110)$$

and

$$|a_2| \lesssim m^2/s_{12}, \quad k_{2\perp}^2 \lesssim m^2, \quad (111)$$

while b_2 remains free at this stage.

Next we examine all the invariant energies across the Reggeons and require them to be $\gg m^2$.

Reggeon with α_1 :

$$(k_3 - l_1)^2 \approx a_3(-B_1)s_{12}, \quad (112)$$

Reggeon with α_2 :

$$(p_1 - k_3 - l_3)^2 \approx (1 - a_3)(-B_3)s_{12}, \quad (113)$$

Reggeon with α_3 :

$$(k_4 + l_2)^2 \approx b_4 A_2 s_{12}, \quad (114)$$

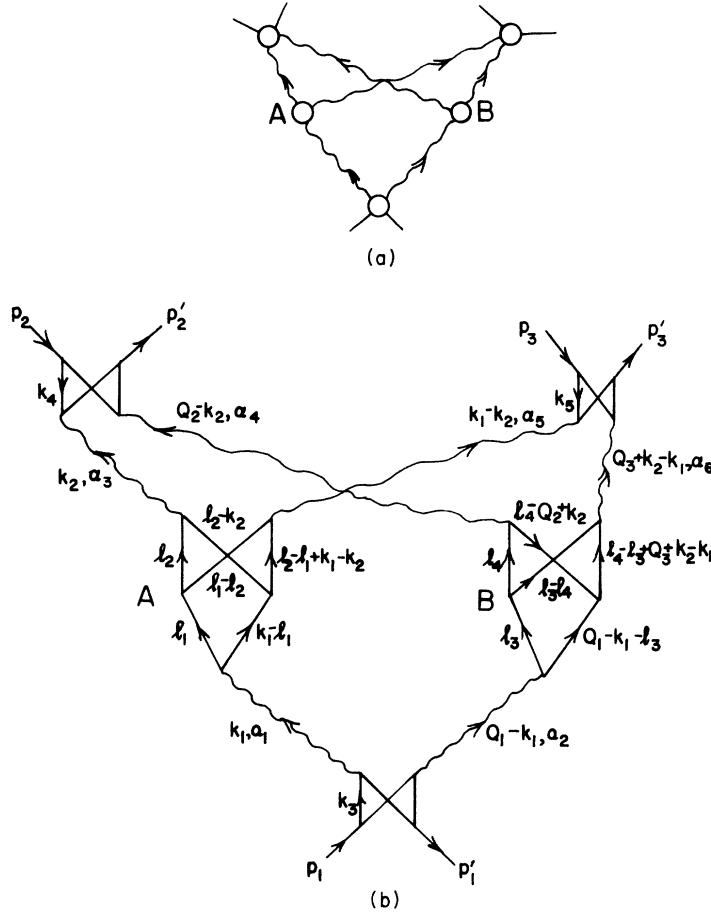


FIG. 14. (a) The Reggeon graph involving the double cross. This graph contains two branching vertices A and B . At either one, one may have energy nonconservation. (b) The hybrid field-theory graph used to study the structure of the double crossed graph.

Reggeon with α_4 :

$$(p_2 - k_4 + l_4)^2 \approx (1 - b_4)A_4 s_{12}, \quad (115)$$

Reggeon with α_5 :

$$(k_5 + l_1 - l_2)^2 \approx b_5(A_1 - A_2)s_{12}, \quad (116)$$

and

Reggeon with α_6 :

$$(p_3 - k_5 + l_3 - l_4)^2 \approx (R - b_5)(A_3 - A_4)s_{12}. \quad (117)$$

These are large only if

$$|a_3|, |b_3|, |b_5| \gg m^2/s_{12}, \quad (118)$$

and

$$|B_1|, |B_3|, |A_2|, |A_4|, |A_1 - A_2|, |A_3 - A_4| \gg m^2/s_{12}. \quad (119)$$

Now by using these restrictions we find that the lower vertex is independent of a_1 and a_2 , but depends on b_1 . The upper left depends on a_1 , but not

b_1 ; the upper right depends on $a_2 - a_1$, but not b_1 .

We have yet to learn about the size of b_2 . To determine this we examine those denominators of the vertices A and B which may depend on a_1, a_2, b_1 , or b_2 . Using our restrictions found so far we note for vertex A that

$$(k_1 - l_1)^2 - m^2 \approx s_{12}A_1B_1 + (k_1 - l_1)_\perp^2 - m^2, \quad (120)$$

$$(l_2 - l_1 + k_1 - k_2)^2 - m^2 \approx s_{12}(A_2 - A_1)(B_2 - B_1 - b_2) + (l_2 - l_1 + k_1 - k_2)_\perp^2 - m^2, \quad (121)$$

and

$$(l_2 - k_2)^2 - m^2 \approx s_{12}A_2(B_2 - b_2) + (l_2 - k_2)_\perp^2 - m^2, \quad (122)$$

and for vertex B that

$$(Q_1 - k_1 - l_3)^2 - m^2 \approx s_{12}A_3B_3 + (Q_1 - k_1 - l_3)_\perp^2 - m^2, \quad (123)$$

$$\begin{aligned}
& (l_4 - l_3 + Q_3 + k_2 - k_1)^2 - m^2 \\
& \approx s_{12}(A_4 - A_3) \left(B_4 - B_3 + b_2 + \frac{s_{\perp}}{s_{12}} \right) \\
& + (l_4 - l_3 + Q_3 + k_2 - k_1)_{\perp}^2 - m^2, \quad (124)
\end{aligned}$$

and

$$\begin{aligned}
& (l_4 + k_2 - Q_2)^2 - m^2 \approx s_{12}A_4 \left(B_4 + b_2 + \frac{s_{\perp}}{s_{12}} \right) \\
& + (l_4 + k_2 - Q_2)_{\perp}^2 - m^2. \quad (125)
\end{aligned}$$

And here we see the appearance of the crucial quantity s_1/s_{12} . If $|b_2| \gg s_1/s_{12}$, we may drop s_1/s_{12} in vertex B and our amplitude would be independent of s_1 . It must then contribute to the three terms of T_6 having no discontinuity in s_1 and is, thus, of no interest to us. We learn then

$$\frac{m^2}{s_{12}} \lesssim |b_2| \lesssim \frac{s_1}{s_{12}}. \quad (126)$$

With this we see that the upper vertices do not depend on b_2 because the b_4 and b_5 parameters are of

order 1 and much greater than s_1/s_{12} .

These observations allow us to split the b_2 integration into two pieces; piece I,

$$m^2/s_{12} \lesssim |b_2| \ll s_1/s_{12}, \quad (127)$$

and piece II,

$$|b_2| \approx s_1/s_{12},$$

such that

$$\frac{m^2}{s_{12}} \lesssim \left| b_2 + \frac{s_1}{s_{12}} \right| \ll \frac{s_1}{s_{12}}. \quad (128)$$

In piece I we may neglect b_2 in vertex B . In piece II we change variables to $\tilde{b}_2 = b_2 + s_1/s_{12}$ and neglect \tilde{b}_2 in vertex A .

In region I we then have that the lower vertex contains all the b_1 dependence, the upper left vertex depends on a_2 only, the upper right vertex depends on $a_2 - a_1$ only, the vertex A contains all the b_2 dependence, and B depends on none of a_1 , a_2 , b_1 , or b_2 . The amplitude for Fig. 14(b) splits as

$$\begin{aligned}
T_6 = & \frac{i|s_{12}|^2}{4(2\pi)^8} \int d^2k_{1\perp} d^2k_{2\perp} s_{12}^{\alpha_1 + \dots + \alpha_6} \xi_{\alpha_1} \dots \xi_{\alpha_6} \\
& \times \frac{g^2|s_{12}|^2}{4(2\pi)^8} \int db_2 \int \frac{dA_1 dB_1 d^2l_{1\perp} dA_2 dB_2 d^2l_{2\perp} (-B_1)^{\alpha_1} A_2^{\alpha_3} (A_1 - A_2)^{\alpha_5} \beta^3}{D_{A_1} \dots D_{A_6}} \\
& \times \frac{g^2|s_{12}|^2}{4(2\pi)^8} \int \frac{dA_3 dB_3 d^2l_{3\perp} dA_4 dB_4 d^2l_{4\perp} (-B_3)^{\alpha_2} A_4^{\alpha_4} (A_3 - A_4)^{\alpha_6} \beta^3}{D_{B_1} \dots D_{B_6}} \\
& \times \frac{g^2|s_{12}|}{2(2\pi)^4} \int \frac{db_1 da_3 db_3 d^2k_{3\perp} (1 - a_3)^{\alpha_2} a_3^{\alpha_1} \beta^2}{D_{L_1} \dots D_{L_4}} \\
& \times \frac{g^2|s_{12}|}{2(2\pi)^4} \int da_2 da_4 db_4 \frac{d^2k_{4\perp} (1 - b_4)^{\alpha_4} b_4^{\alpha_3} \beta^2}{D_{UL_1} \dots D_{UL_4}} \\
& \times \frac{g^2|s_{12}|}{2(2\pi)^4} \int d(a_2 - a_1) da_5 db_5 d^2k_{5\perp} \frac{(R - b_5)^{\alpha_6} b_5^{\alpha_5} \beta^2}{D_{UR_1} \dots D_{UR_4}}, \quad (129)
\end{aligned}$$

where the various denominators have been labeled D_{UR} for upper right, etc. Needless to say, we may markedly simplify (129) by noting that various blocks are just $N_{\alpha_i \alpha_j}$ or $r_{\alpha_i, \alpha_j, \alpha_k}$. For example, we see that the lower- and upper-left integrals are just $(|s_{12}|/\sqrt{2}2\pi) N_{\alpha_1 \alpha_2}$ and $(|s_{12}|/\sqrt{2}2\pi) N_{\alpha_3 \alpha_4}$, respectively. By scaling b_5 we see that the upper-right vertex is $R^{\alpha_5 + \alpha_6 + 1} (|s_{13}|/\sqrt{2}2\pi) N_{\alpha_5 \alpha_6}$. Vertex B is also easy to handle since it is exactly the same as we encountered for r before, and we note

$$\xi_{\alpha_2} \xi_{\alpha_4} \xi_{\alpha_6} s_{12}^{\alpha_4} s_{12}^{\alpha_6} s_{12}^{\alpha_6} \times \text{integral over vertex } B = -\xi_{\alpha_4} \xi_{\alpha_6} \xi_{\alpha_2 - \alpha_4 - \alpha_6} s_{12}^{\alpha_4} s_{12}^{\alpha_6} s_{12}^{\alpha_2 - \alpha_4 - \alpha_6} r_{\alpha_2, \alpha_4, \alpha_6}. \quad (130)$$

The integral over vertex A requires a little more doing. Scale the variables as $b_2 = s_1/s_{12} \tilde{b}_2$, $B_1 = s_1/s_{12} \tilde{B}_1$, $\tilde{B}_2 = s_1/s_{12} \tilde{B}_2$, so the range of \tilde{b}_2 is

$$m^2/s_1 \lesssim |\tilde{b}_2| \ll 1, \quad (131)$$

while the range of integration on A_1 and A_2 is

$$m^2/s_1 \ll |A_1|, |A_2| \ll 1. \quad (132)$$

Recalling one's experience¹⁴ with the triple-Reggeon vertex of Fig. 15, we note

$$\frac{\xi_{\alpha_1}}{\sqrt{2}(2\pi)} \times \text{integral for vertex } A = \frac{i}{s_{12}} \frac{s_1^{\alpha_1 - (\alpha_3 + \alpha_5 - 1)} - 1}{\alpha_1 - (\alpha_3 + \alpha_5 - 1)} \gamma_{\alpha_1, \alpha_3, \alpha_5}. \tag{133}$$

Putting together all these simplifications we reach

$$T_6(\text{region I of Fig. 14(b)}) = \int \frac{d^2k_{1\perp}}{(2\pi)^2} \frac{d^2k_{2\perp}}{(2\pi)^2} \xi_{\alpha_4} \xi_{\alpha_6} \xi_{\alpha_3} \xi_{\alpha_5} \xi_{\alpha_2 - \alpha_4 - \alpha_6} s_{12}^{\alpha_3 + \alpha_4 - 1} s_{13}^{\alpha_5 + \alpha_6 - 1} s_1^{\alpha_2 - \alpha_4 - \alpha_6} \frac{s_1^{\alpha_1 - (\alpha_3 + \alpha_5 - 1)} - 1}{\alpha_1 - (\alpha_3 + \alpha_5 - 1)} \\ \times N_{\alpha_1 \alpha_2} N_{\alpha_3 \alpha_4} N_{\alpha_5 \alpha_6} \gamma_{\alpha_1, \alpha_3, \alpha_5} \gamma_{\alpha_2, \alpha_4, \alpha_6}. \tag{134}$$

The study of region II proceeds just as above and results in the same integral as (134) with the replacement

$$\xi_{\alpha_2 - \alpha_4 - \alpha_6} s_1^{\alpha_2 - \alpha_4 - \alpha_6} \frac{s_1^{\alpha_1 - (\alpha_3 + \alpha_5 - 1)} - 1}{\alpha_1 - (\alpha_3 + \alpha_5 - 1)} \rightarrow \xi_{\alpha_1 - \alpha_3 - \alpha_5} s_1^{\alpha_1 - \alpha_3 - \alpha_5} \frac{s_1^{\alpha_2 - (\alpha_4 + \alpha_6 - 1)} - 1}{\alpha_2 - (\alpha_4 + \alpha_6 - 1)}. \tag{135}$$

Introducing angular momenta l_1, \dots, l_6 for each Reggeon we are able to evaluate the partial-wave amplitudes for regions I and II,

$$F_I(J_i, t_i) = \int \frac{d^2k_{1\perp} d^2k_{2\perp} dl_1 \dots dl_6}{(2\pi)^4 (2\pi i)^6} N_{l_1 l_2} N_{l_3 l_4} \gamma_{l_3 l_4} N_{l_5 l_6} \gamma_{l_5 l_6} \gamma_{l_1, l_3, l_5} \gamma_{l_2, l_4, l_6} G_{l_1}(\alpha_1) \dots G_{l_6}(\alpha_6) \\ \times \frac{1}{J_2 - (l_3 + l_4 - 1)} \frac{1}{J_3 - (l_5 + l_6 - 1)} \frac{1}{J_1 - (l_1 + l_2 - 1)} \frac{1}{J_1 - (l_3 + l_2 + l_5 - 2)}, \tag{136}$$

and

$$F_{II}(J_i, t_i) = \int \frac{d^2k_{1\perp} d^2k_{2\perp} dl_1 \dots dl_6}{(2\pi)^4 (2\pi i)^6} N_{l_1 l_2} N_{l_3 l_4} \gamma_{l_3 l_4} N_{l_5 l_6} \gamma_{l_5 l_6} \gamma_{l_1, l_3, l_5} \gamma_{l_2, l_4, l_6} G_{l_1}(\alpha_1) \dots G_{l_6}(\alpha_6) \\ \times \frac{1}{J_2 - (l_3 + l_4 - 1)} \frac{1}{J_3 - (l_5 + l_6 - 1)} \frac{1}{J_1 - (l_1 + l_2 - 1)} \frac{1}{J_1 - (l_1 + l_4 + l_6 - 2)}. \tag{137}$$

In the next section we will use these results to derive our Reggeon graph technique. Here we finish by noting the important presences of $\gamma_{l_3 l_4}$ and $\gamma_{l_5 l_6}$ which provide zeroes at physical J_2 and J_3 , respectively, thus decoupling this graph and its branch points from physical partial waves.

VI. FORMULATION OF THE DIAGRAM RULES

We are now prepared to translate our results from the analysis of the hybrid graphs into rules for the equivalent Reggeon diagrams. To facilitate this transcription we define the usual Reggeon energies⁴

$$E = 1 - \text{angular momentum.} \tag{138}$$

The relation between $T_6(s_{12}, s_{13}, s_1, t_1)$ and $F(J_i, t_i)$ becomes

$$\frac{s_{12} s_{13}}{s_1} T_6 = \int_{c-i\infty}^{c+i\infty} \frac{dE_1 dE_2 dE_3}{(2\pi i)^3} \xi_{J_1 - J_2 - J_3} \xi_{J_2} \xi_{J_3} \\ \times \exp[-(E_1 \tau_1 + E_2 \tau_2 + E_3 \tau_3)] \\ \times F(E_i, t_i), \tag{139}$$

where the "times" conjugate to the energies E_i are

$$\tau_1 = \ln s_1, \tag{140}$$

$$\tau_2 = \ln(s_{12}/s_1), \tag{141}$$

and

$$\tau_3 = \ln(s_{13}/s_1), \tag{142}$$

and the E_i contours run to the left of singularities in F . With this notation the partial-wave amplitude for region I of Fig. 14(b), Eq. (136), becomes (see Fig. 16)

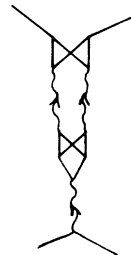


FIG. 15. The hybrid graph contribution to the elastic amplitude where the two-particle-two-Reggeon function N and the energy-conserving triple-Reggeon vertex appears.

$$\begin{aligned}
F(\text{region I, Fig. 14(b)}) &= \int \frac{d^2k_{1\perp} d^2k_{2\perp} \cdots d^2k_{6\perp}}{(4\pi^2)^6} (2\pi)^2 \delta^2(Q_2 - k_3 - k_4) (2\pi)^2 \delta^2(Q_3 - k_5 - k_6) (2\pi)^2 \delta^2(Q_1 - k_1 - k_2) \\
&\quad \times (2\pi)^2 \delta^2(k_1 - k_3 - k_5) (2\pi)^2 \delta^2(k_2 - k_4 - k_6) NNN \gamma \gamma \gamma_{\epsilon_1, \epsilon_3, \epsilon_5} \gamma_{\epsilon_2, \epsilon_4, \epsilon_6} G(\epsilon_1, k_{1\perp}) \cdots G(\epsilon_6, k_{6\perp}) \\
&\quad \times \frac{1}{E_1 - \epsilon_1 - \epsilon_2} \frac{1}{E_1 - \epsilon_3 - \epsilon_5 - \epsilon_2} \frac{1}{E_2 - \epsilon_3 - \epsilon_4} \frac{1}{E_3 - \epsilon_5 - \epsilon_6}, \tag{143}
\end{aligned}$$

where

$$G(\epsilon_i, k_{j\perp}) = \frac{1}{\epsilon_i - [1 - \alpha(k_{j\perp})]}, \tag{144}$$

and $\epsilon_i = 1 - l_i$.

This result has its natural interpretation in terms of "old-fashioned" perturbation theory where *momentum is conserved, but not energy* at each step. The progress of energy is represented by the energy denominators in (143) which give the total energy E_i in channels 1, 2, or 3 minus the energy of the propagating quasiparticles at each step of the interaction. These steps, which correspond to different time stages, are shown as the dashed intermediate lines in Fig. 16. For region II of the double crossed graph one has vertex B involving Reggeons 2, 4, and 6 occurring "before" A , and the Reggeon energy denominators are, as we read from Fig. 17,

$$\frac{1}{E_1 - \epsilon_1 - \epsilon_2} \frac{1}{E_1 - \epsilon_1 - \epsilon_4 - \epsilon_6} \frac{1}{E_2 - \epsilon_3 - \epsilon_4} \frac{1}{E_3 - \epsilon_5 - \epsilon_6}, \tag{145}$$

which is consistent with Eq. (137).

How are we to interpret this result? A very attractive formulation is to focus our attention on the "time" variables involved. In the triple-Regge

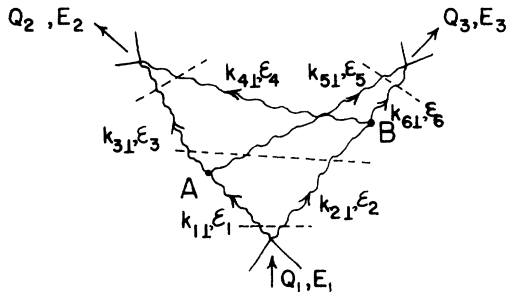


FIG. 16. The time ordering appropriate to the old-fashioned perturbation theory interpretation of the partial-wave amplitude of Fig. 14, region I. The time (rapidity) runs upward. The time in vertex B is later than in vertex A . Each of the dashed lines corresponds to an energy denominator. In this figure we read off the energy denominators to be

$$\begin{aligned}
&[(E_1 - \epsilon_1 - \epsilon_2) (E_1 - \epsilon_3 - \epsilon_5 - \epsilon_2) \\
&\quad \times (E_2 - \epsilon_3 - \epsilon_4) (E_3 - \epsilon_5 - \epsilon_6)]^{-1}.
\end{aligned}$$

graphs we have considered there are four times we have distinguished. They are as follows: First, the time the lower vertex with energy E_1 and two-momentum \vec{Q}_1 emits Reggeons. This time is $\eta_0 = 0$ in our examples. Next is the time at which the energy-nonconserving interaction takes place,

$$\eta_1 = \ln s_1; \tag{146}$$

then is the time at which energy E_2 and momentum \vec{Q}_2 leave the interaction,

$$\eta_2 = \ln s_{12}; \tag{147}$$

and then the time when energy E_3 and momentum \vec{Q}_3 leave,

$$\eta_3 = \ln s_{13}. \tag{148}$$

All energies s_1 , s_{12} , and s_{13} are to be given in some convenient units, say the common mass of the problem, m^2 . If we consider energy $E_1 - E_2 - E_3$ to be lost at time η_1 , then the amplitude in time space depends only on

$$\begin{aligned}
\tau_1 &= \eta_1 - \eta_0 \\
&= \ln s_1, \\
\tau_2 &= \eta_2 - \eta_1 \\
&= \ln \frac{s_{12}}{s_1}, \\
\tau_3 &= \eta_3 - \eta_1 \\
&= \ln \frac{s_{13}}{s_1}.
\end{aligned} \tag{149}$$

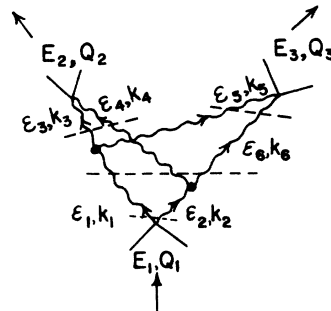


FIG. 17. The same as Fig. 16, except it is for region II of the integration for the hybrid graph of Fig. 14. The time of A is now later than that of vertex B .

Now these times are just the rapidities associated with any given vertex or momentum at that vertex. For a vector

$$v = a_v \tilde{p}_1 + b_v \tilde{p}_2 + v_\perp, \tag{149}$$

we may define the time

$$\begin{aligned} \tau_v &= \ln \frac{2\tilde{p}_1 \cdot v}{m} \\ &= \ln b_v \frac{s_{12}}{m^2}. \end{aligned} \tag{150}$$

In the double crossed graph in region I, the range of the momenta at the *A* vertex is such that the times in *A* are between 0 and τ_1 , while in the *B* vertex the times are of order τ_1 . These time assignments switch when we go over to region II of the double cross. This suggests that we ought to be able to write the double crossed graph for region I as an integral over the time of vertex *A* which ranges only from zero to τ_1 . That is, if we define the *time-momentum-space* expression of the partial-wave amplitude $F(E_i, \vec{Q}_i)$ by

$$F(E_i, \vec{Q}_i) = \int_0^\infty d\tau_1 \int_0^\infty d\tau_2 \int_0^\infty d\tau_3 e^{\tau_1 E_1 + \tau_2 E_2 + \tau_3 E_3} H(\tau_1, \tau_2, \tau_3, \vec{Q}_i), \tag{151}$$

then $H(\tau_i, \vec{Q}_i)$ ought to have a simple expression in terms of propagators for the Reggeons

$$G_a(\vec{Q}, \tau) = e^{-\tau \epsilon_a(\vec{Q})} \theta(\tau) \tag{152}$$

and restricted time integrals. For region I of the double crossed graph we write (as in Fig. 18)

$$\begin{aligned} H(\tau_1, \tau_2, \tau_3) &= \int \frac{d^2 k_1 d^2 k_3}{(2\pi)^4} \int_0^{\eta_1} d\eta G_1(\vec{k}_1, \eta) G_3(\vec{k}_3, \eta_2 - \eta) G_5(\vec{k}_1 - \vec{k}_3, \eta_3 - \eta) G_2(\vec{Q}_1 - \vec{k}_1, \eta_1) G_6(\vec{Q}_3 + \vec{k}_3 - \vec{k}_1, \eta_3 - \eta_1) \\ &\quad \times G_4(\vec{Q}_2 - \vec{k}_3, \eta_2 - \eta_1) N_{\epsilon_3 \epsilon_4} \gamma_{\epsilon_3 \epsilon_4} N_{\epsilon_5 \epsilon_6} \gamma_{\epsilon_5 \epsilon_6} N_{\epsilon_1 \epsilon_2} \gamma_{\epsilon_1 \epsilon_2} \gamma_{\epsilon_1 \epsilon_3 \epsilon_5} \gamma_{\epsilon_2 \epsilon_4 \epsilon_6}. \end{aligned} \tag{153}$$

Using (152) for $G_a(\vec{Q}, \eta)$ and $\eta_1 = \tau_1$, $\eta_2 = \tau_2 + \tau_1$, and $\eta_3 = \tau_3 + \tau_1$ we find (143) for $F(E_i, \vec{Q}_i)$.

A general prescription is given in pictures in Fig. 19. One locates four times $\eta_0 = 0$, η_1 , η_2 , and η_3 on a time axis. All Reggeon interactions before η_1 are restricted in time integration to be $\leq \eta_1$. This will all be interactions in channel 1. Some of these interactions will have their time integrations automatically restricted by the step function $\theta(\eta)$ in (152). Others, as in the double cross will have their times restricted by hand. All interactions after η_1 occur only in channel 2 or in channel

3. After η_1 there is no interaction between channels 2 and 3. In the case of a graph like the double crossed graph or its generalizations (Fig. 20) one will find two or more three-Reggeon vertices whose time variable is not restricted by θ functions alone. One must choose these one at a time and note them with the time $\eta_1 = \ln s_1$. The others have their time integration restricted to be $\leq \eta_1$. This gives directly the two terms of the double crossed graph and k terms in a graph with k such vertices.

We can also give energy-momentum space rules

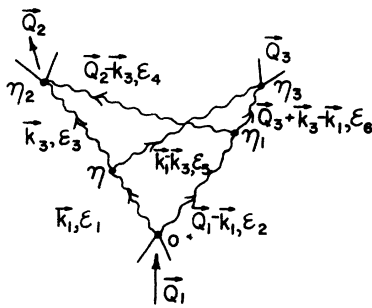


FIG. 18. The time-momentum-space Reggeon graph for the double crossed hybrid diagram. The times are $\eta_0 = 0$, $\eta_1 = \ln s_1$, $\eta_2 = \ln s_{12}$, and $\eta_3 = \ln s_{13}$. The intermediate time η is integrated over $0 \leq \eta \leq \eta_1$.

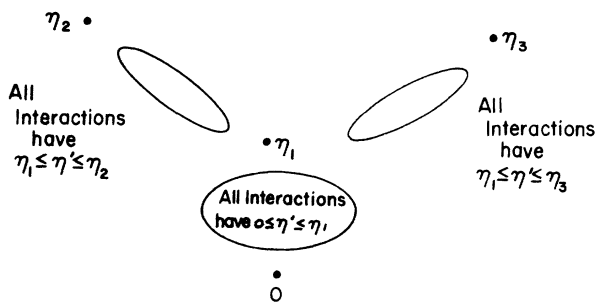


FIG. 19. The "time" space classification of all allowed Reggeon graphs. After η_1 there is no interaction between the Reggeons going up to η_2 and those progressing toward η_3 . The time η_1 always occurs at a branching vertex.

for each Reggeon graph. To do this we first rotate the energy contours by $\frac{1}{2}\pi$ to the real axis. The propagator becomes

$$G_a(\epsilon, \vec{q}) = \frac{i}{\epsilon - [1 - \alpha_a(\vec{q})] + i\delta} \quad (154)$$

instead of (144). Introducing the δ^\pm functions

$$\delta^\pm(x) = \frac{\mp 1}{2\pi i} \frac{1}{x \pm i\delta}, \quad (155)$$

$$\delta^+(x) + \delta^-(x) = \delta(x), \quad (156)$$

we may write the partial-wave amplitude for region I of the double crossed graph, Eq. (143), as

$$\begin{aligned} F_1(E_1, \vec{Q}_1) = & \int \frac{d^2k_1 \cdots d^2k_a}{(4\pi^2)^a} (2\pi)^2 \delta^2(\vec{Q}_2 - \vec{k}_3 - \vec{k}_4) (2\pi)^2 \delta^2(\vec{Q}_3 - \vec{k}_5 - \vec{k}_6) (2\pi)^2 \delta^2(\vec{Q}_1 - \vec{k}_1 - \vec{k}_2) (2\pi)^2 \delta^2(\vec{k}_1 - \vec{k}_3 - \vec{k}_5) \\ & \times (2\pi)^2 \delta^2(\vec{k}_2 - \vec{k}_4 - \vec{k}_6) \int \frac{d\omega_1 \cdots d\omega_a}{(2\pi)^a} G_1(\omega_1, \vec{k}_1) \cdots G_a(\omega_a, \vec{k}_a) N_{\omega_1 \omega_2} (2\pi) \delta(E_1 - \omega_1 - \omega_2) \\ & \times N_{\omega_3 \omega_4} \gamma_{\omega_3 \omega_4} (2\pi) \delta(E_2 - \omega_3 - \omega_4) N_{\omega_5 \omega_6} \gamma_{\omega_5 \omega_6} (2\pi) \delta(E_3 - \omega_5 - \omega_6) \\ & \times \gamma_{\omega_1, \omega_3, \omega_5} (2\pi) \delta^+(\omega_1 - \omega_3 - \omega_5) \gamma_{\omega_2, \omega_4, \omega_6}. \end{aligned} \quad (157)$$

For region II we make the replacement

$$\delta^+(\omega_1 - \omega_3 - \omega_5) \rightarrow \delta^+(\omega_2 - \omega_4 - \omega_6). \quad (158)$$

When $E_1 = E_2 + E_3$, that is, over-all energy is conserved, the sum of regions I and II reproduces exactly the contribution of the double cross to the two-to-two amplitude, as it ought.

In energy-momentum space our Reggeon rules are begun by stating the criterion for a vertex where energy may not be conserved. Basically, it is a vertex whose time integration is not restricted by the $\theta(\eta)$ in Green's functions. We call such a vertex a *branching vertex*. We give two kinds of definitions for these vertices.

Definition I.

(a) A *possible* branching vertex has one line entering from an earlier time and two departing to a later time.

(b) Identify all possible branching vertices.

(c) If a possible branching vertex has its time restricted by another possible vertex, it is not a branching vertex.

(d) The remaining possible branching vertices, are actually branching vertices.

Definition II.

(a) It has two outgoing Reggeon lines.

(b) If we leave the vertex along one outgoing line, we do not meet any Reggeon lines connected via

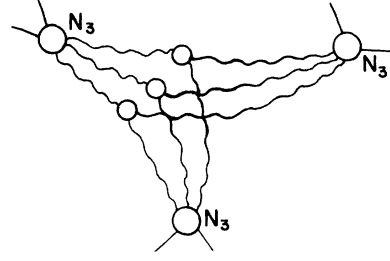


FIG. 20. A Reggeon graph with three branching vertices. This graph gives *three* contributions to $F(E_1, \vec{Q}_1)$. Each of the branching vertices is noted in turn. Energy nonconservation occurs there. The noted branching vertex will carry time η_1 ; the time integrations in the other branching vertices will run up to η_1 . In energy space the noted branching vertex receives a factor of 1; the other branching vertices receive a δ^+ function.

interactions (none, one, ...) to the other outgoing line.

Also:

(a) Each line of a graph carries energy ϵ and momentum \vec{k} . Associate with each Reggeon a propagator

$$G_{\vec{k}}(\epsilon, k) = i\{\epsilon - [1 - \alpha_a(\vec{k})] + i\delta\}^{-1}. \quad (159)$$

(b) At each vertex where three Reggeons meet, place the triple-Regge vertex $\gamma_{\omega_1, \omega_2, \omega_3}$. If energy is conserved at that vertex, place a $2\pi \delta(\omega_1 - \omega_2 - \omega_3)$. In a graph with k branching vertices select them one at a time. The selected vertex does not conserve energy and receives a factor of unity. At the $k - 1$ other branching vertices put a $\delta^+(\omega_{in} - \sum \omega_{out})$ in momentum space or restrict their time integrations by $\eta_1 = \ln s_1$, the time of the selected vertex.

(c) Two-momentum is conserved at each vertex.

(d) Energy E_1 and momentum \vec{Q}_1 , $t_1 = -|\vec{Q}_1|^2$, enters the graph at the bottom (time zero) where two particles create n_1 Reggeons via a function $N_{n_1}(E_1, \vec{Q}_1; \epsilon_i, \vec{k}_1, \dots, \epsilon_{n_1}, \vec{k}_{n_1})$. Energy and momentum are conserved here. n_j Reggeons depart via an N_{n_j} function carrying off E_j and \vec{Q}_j ; $j=2$ and 3 .

(e) All Reggeon energies and momenta are to be integrated, $\int d^2k d\epsilon / (2\pi)^3$.

(f) At each vertex with $n \geq 2$ Reggeons coming

from below put a factor $\gamma_{\epsilon_1} \dots \epsilon_n$,^{4,14} the generalization of $\gamma_{\epsilon_1 \epsilon_2}$.

Finally we complete the diagram rules by telling how the triple-Regge inclusive cross section $a+b \rightarrow c$ + anything is gotten from our $F(J_i, \vec{Q}_i)$ constructed by the instruction just given. The reaction is shown in Fig. 21. In terms of our variables we want the limit $s_{12} = s + i\epsilon$, $s_{13} = s - i\epsilon$, $t_1 = 0$, $t_2 = t_3 = t$, and the discontinuity in $s_1 = M^2$,

$$s^2 \frac{do(a+b \rightarrow c+X)}{dt dM^2} = \int \frac{dJ_1 dJ_2 dJ_3}{(2\pi i)^3} \xi_{J_2} \xi_{J_3}^* \left(\frac{s}{M^2} \right)^{J_2+J_3} (M^2)^{J_1} F(J_1, J_2, J_3, t_1=0, t_2=t, t_3=t). \quad (160)$$

VII. REGGEON FIELD THEORY FOR THE TRIPLE-REGGE AMPLITUDE AND RENORMALIZATION

The diagram technique we have described finds its most interesting application in the study of the triple-Pomeron (P) vertex and the P corrections to that vertex. As is well known, the P involves a Reggeon with $\alpha(0)=1$, and, therefore, branch points of multiple- P exchange in any of the J_i channels pile up at $t_i=0$. Since it is precisely the behavior at $t_1=t_2=t_3=0$ that caused the interest in the triple- P vertex, the formalism we have developed here applies. We, furthermore, can concentrate our attention on all J_i near unity and all $t_i = -|\vec{Q}_i|^2$ near zero. From Refs. 4, 9, and 10 we know that to study the most important structure in this region we need concentrate only on local triple- P couplings since quartic and higher and derivative couplings are negligible. Furthermore, noting that each $\gamma_{t_1 t_2} = -1$ in this regime, we are able to associate a factor i with each triple- P vertex except the energy-nonconserving vertex.

In the case of all graphs conserving energy and momentum the counting is straightforward and is given in Ref. 9 and 10. Here we must account for energy nonconservation as well. Our attention is focused on the one- P to two- P proper vertex function $\tilde{\Gamma}^{(1,2)}(E_1, E_2, E_3, \vec{Q}_1, \vec{Q}_2, \vec{Q}_3)$, which is the generalization of the energy conserving $\Gamma^{(1,2)}$ of Ref. 10. Of course, we must have

$$\tilde{\Gamma}^{(1,2)}|_{E_1=E_2+E_3} = \Gamma^{(1,2)}. \quad (161)$$

Now $\tilde{\Gamma}^{(1,2)}$ is given as an infinite sum over three- P proper vertices with 1, 2, ... branching vertices

$$\tilde{\Gamma}^{(1,2)} = \sum_{k=1}^{\infty} k \Gamma_k^{(1,2)}, \quad (162)$$

where $\Gamma_k^{(1,2)}$ is the one- P to two- P proper vertex with k branching vertices. Skeleton expansions can be given for $\Gamma_k^{(1,2)}$. Some terms of these for

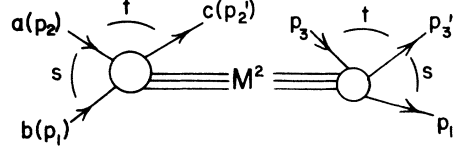


FIG. 21. The inclusive cross section $p_1 + p_2 \rightarrow p'_2 + X$. It is related to our six-point amplitude by Eq. (160).

$k=1$ and 2 are shown in Figs. 22 and 23. Note that the basic building blocks of $\tilde{\Gamma}^{(1,2)}$ are the energy-conserving $\Gamma^{(1,2)}$ and the vertex $\Gamma_1^{(1,2)}$ with one branching vertex. The appearance of the weight factor k in (162) is familiar from the extensive discussion of the double crossed graph in previous sections.

Now the renormalization procedure will go through as before,^{9,10} with the one change being that an additional normalization function will be needed for the energy-nonconserving coupling. We encounter here an amusing complication which does not allow us to proceed in any easy manner to the detailed behavior of the triple-Regge inclusive cross section (160) as a function of s , t , and M^2 . In the renormalization-group analyses of Refs. 4, 9, and 10 one is able to give arguments concerning the general scaling form of functions such as $F(E_i, \vec{Q}_i)$. Such scaling laws in themselves are not enough here, interesting as they may be. We need much more knowledge of the precise behavior of the scaling functions on their scaled arguments before we can extract the information we desire. The techniques for doing precisely this are derived in a subsequent paper. We end this long exposition with both contenting ourselves at having achieved our diagram technique and encouraging the hearty reader to proceed to the next section.

VIII. CONCLUSION AND SUMMARY

In this paper we have derived a set of rules for the evaluation of Regge-pole and branch-cut contributions to the six-point scattering amplitude in the triple-Regge region. Referring to the kinematics in Fig. 1 we showed that in the triple-Regge limit

$$s_{12}, s_{13}, s_1 \rightarrow \infty, \quad \frac{s_{12}}{s_1}, \frac{s_{13}}{s_1} \rightarrow \infty, \quad (163)$$

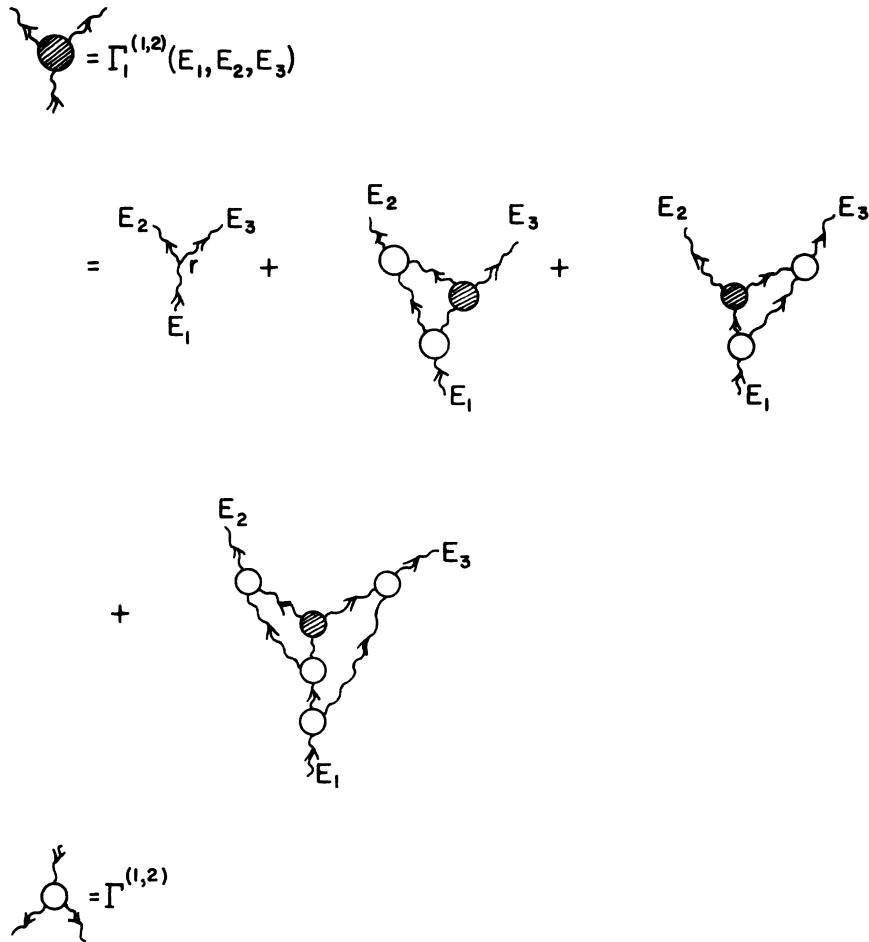


FIG. 22. The skeleton expansion for the proper three-Reggeon amplitude with one branching vertex, $\Gamma_1^{(1,2)}$. It involves $\Gamma_1^{(1,2)}$ itself and the energy-conserving proper three-Reggeon vertex $\Gamma^{(1,2)}$ used in Ref. 10. All propagators are full.

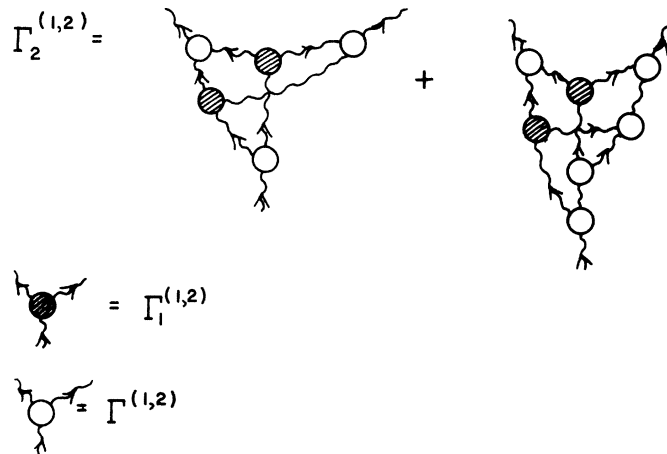


FIG. 23. The skeleton expansion for the proper $\Gamma_2^{(1,2)}$. It involves $\Gamma_1^{(1,2)}$ and $\Gamma^{(1,2)}$. All propagators are full.

$$\frac{s_{12}}{s_{13}}, t_i \text{ fixed;} \quad (164)$$

the six-point amplitude may be represented as

$$T_6(s_{12}, s_{13}, s_1, t_i) = \int_{c-i\infty}^{c+i\infty} \frac{dJ_1 dJ_2 dJ_3}{(2\pi i)^3} s_{12}^{J_2} s_{13}^{J_3} s_1^{J_1} s_1^{-J_2-J_3} \times \xi_{J_2} \xi_{J_3} \xi_{J_1-J_2-J_3} F(J_1, J_2, J_3, t_i), \quad (165)$$

where

$$\frac{s^2 d\sigma(p_1+p_2-p'_2+X)}{dt dM^2} = \frac{1}{2i} \text{disc}_{s_1=M^2} T_6(s_{12}=s+i\epsilon, s_{13}=s-i\epsilon, s_1=M^2, t_1=0, t_2=t_3=t). \quad (168)$$

With the phase factors ξ removed, the partial-wave amplitude is real analytic. Our rules tell how to evaluate it.

The function $F(J_i, t_i)$ is very much like a three-Reggeon Green's function in conventional Reggeon field theory^{4,9,10} except that Reggeon energy $E_i = 1 - J_i$ is not conserved. This is due to the fact that we have singled out a special "time" (rapidity) $\eta_1 = \ln s_1$ in the progression of Reggeons from their emission at time $\eta_0 = 0$ where they emerge from a two-particle source with net Reggeon energy E_1 and net two-momentum Q_1 ($t_1 = -|Q_1|^2$) to their absorption at time $\eta_2 = \ln s_{12}$ or $\eta_3 = \ln s_{13}$. If we integrate over this time η_1 setting $\eta_2 = \eta_3$, we recover energy conservation and the appropriate form for Reggeon-graph contributions to the $2 \rightarrow 2$ amplitude with net rapidity $Y = \ln s_{12}$.

We have given detailed formulations for the evaluation of $F(E_i, \bar{Q}_i)$ in energy-momentum space and for its time-momentum-space analog $H(\eta_i, \bar{Q}_i)$. Either is convenient for the renormalization-group evaluation of the energy-nonconserving vertices involved. Because a particular intermediate time

$$\xi_{J_i} = \frac{e^{-i\pi J_i + \tau_i}}{\sin \pi J_i} \quad (166)$$

and

$$\xi_{J_1-J_2-J_3} = \frac{e^{-i\pi(J_1-J_2-J_3) + \tau_1\tau_2\tau_3}}{\sin \pi(J_1-J_2-J_3)}, \quad (167)$$

and $\tau_i = \pm 1$ is the signature of a Reggeon in the J_i channel. There are other contributions to T_6 but they do not have a discontinuity in s_1 , the missing mass, and do not contribute to the inclusive cross section

has been prescribed, the counting of graphical contributions to the Reggeon vertex functions is slightly more involved than in the conventional field theory. This is described in Sec. VII.

The renormalization group will give scaling forms for the partial-wave amplitude $F(E_i, \bar{Q}_i)$ in the $E_i \approx 0$, $\bar{Q}_i \approx 0$ limit appropriate, say, for multi-Pomeron contributions to inclusive processes. In order to extract from the triple Sommerfeld-Watson representation, (165), the detailed behavior of inclusive cross sections in s , t , and M^2 , it is necessary to know rather much about the scaling functions themselves. This is done in a subsequent paper²² for reasons of clarity in presentation.

ACKNOWLEDGMENTS

Henry Abarbanel would like to thank Caltech for hospitality while this work was in progress. John Bronzan is indebted to the Theory Group at Fermilab for discussions and opportunities to retreat there to work.

*Operated by Universities Research Association Inc. under contract with the Energy Research and Development Administration.

†Work supported in part by the National Science Foundation under Grant No. MPS 75-06857.

¹S. Mandelstam, *Nuovo Cimento* **30**, 1127 (1963); **30**, 1148 (1963).

²V. N. Gribov, I. Ya. Pomeranchuk, and K. A. Ter-Martirosyan, *Yad. Fiz.* **2**, 361 (1965) [*Sov. J. Nucl. Phys.* **2**, 258 (1966)].

³D. Amati, A. Stanghellini, and S. Fubini, *Nuovo Cimento* **26**, 896 (1962).

⁴This is all reviewed in detail by H. D. I. Abarbanel,

J. B. Bronzan, R. L. Sugar, and A. R. White, *Phys. Rep.* **21C**, 119 (1975), and by H. D. I. Abarbanel, *Rev. Mod. Phys.* (to be published).

⁵J. Finkelstein and K. Kajantie, *Nuovo Cimento* **56A**, 659 (1968).

⁶L. M. Saunders *et al.*, *Phys. Rev. Lett.* **26**, 937 (1971).

⁷C. E. Jones *et al.*, *Phys. Rev. D* **6**, 1033 (1972).

⁸R. Brower and J. Weis, *Phys. Lett.* **41B**, 631 (1972).

⁹A. A. Migdal, A. M. Polyakov, and K. A. Ter-Martirosyan, *Phys. Lett.* **48B**, 239 (1974); *Zh. Eksp. Teor. Fiz.* **67**, 848 (1974) [*Sov. Phys.—JETP* **40**, 420 (1974)].

¹⁰H. D. I. Abarbanel and J. B. Bronzan, *Phys. Rev.*

- D 9, 2397 (1974).
- ¹¹Indeed, J. L. Cardy, R. L. Sugar, and A. R. White [Phys. Lett. 55B, 384 (1975)] have used the Reggeon discontinuity formulas to derive Reggeon rules for the triple-Regge region considered in this paper.
- ¹²J. Bartels, Phys. Rev. D 11, 2977 (1975); 11, 2989 (1975).
- ¹³J. Bartels and E. Rabinovici (unpublished).
- ¹⁴V. N. Gribov, Zh. Eksp. Teor. Fiz 53, 654 (1967) [Sov. Phys.—JETP 26, 414 (1968)].
- ¹⁵H. D. I. Abarbanel and A. Schwimmer, Phys. Rev. D 6, 3018 (1972).
- ¹⁶J. H. Weis, Phys. Rev. D 6, 2823 (1972).
- ¹⁷V. V. Sudakov, Zh. Eksp. Teor. Fiz 30, 87 (1956) [Sov. Phys.—JETP 3, 65 (1956)].
- ¹⁸R. J. Eden, *High Energy Collisions* (Cambridge Univ. Press, New York, 1967) p. 192.
- ¹⁹M. B. Einhorn, J. Ellis, and J. Finkelstein, Phys. Rev. D 5, 2063 (1972).
- ²⁰A. H. Mueller and T. L. Trueman, Phys. Rev. D 5, 2115 (1972).
- ²¹R. Brower, C. E. DeTar, and J. H. Weis, Phys. Rep. 14C, 257 (1974).
- ²²H. D. I. Abarbanel, J. Bartels, J. Bronzan, and D. Sidhu, Phys. Rev. D (to be published).